© 2020. Published by The Company of Biologists Ltd | Journal of Cell Science (2020) 133, jcs246801. doi:10.1242/jcs.246801

RESEARCH ARTICLE

Crumbs, Galla and Xpd are required for Kinesin-5 regulation in mitosis and organ growth in *Drosophila*

Ji-Hyun Hwang‡, Linh Thuong Vuong*,‡ and Kwang-Wook Choi§

ABSTRACT

Xeroderma Pigmentosum D (XPD, also known as ERCC2) is a multi-functional protein involved in transcription, DNA repair and chromosome segregation. In *Drosophila*, Xpd interacts with Crumbs (Crb) and Galla to regulate mitosis during embryogenesis. It is unknown how these proteins are linked to mitosis. Here, we show that Crb, Galla-2 and Xpd regulate nuclear division in the syncytial embryo by interacting with Klp61F, the *Drosophila* mitotic Kinesin-5 associated with bipolar spindles. Crb, Galla-2 and Xpd physically interact with Klp61F and colocalize to mitotic spindles. Knockdown of any of these proteins results in similar mitotic defects. These phenotypes are restored by overexpression of Klp61F, suggesting that Klp61F is a major effector. Mitotic defects of *galla-2 RNAi* are suppressed by Xpd overexpression but not vice versa. Depletion of Crb, Galla-2 or Xpd results in a reduction of Klp61F levels. Reducing proteasome function restores Klp61F levels and suppresses mitotic defects caused by knockdown of Crb, Galla-2 or Xpd. Furthermore, eye growth is regulated by Xpd and Klp61F. Hence, we propose that Crb, Galla-2 and Xpd interact to maintain the level of Klp61F during mitosis and organ growth.

KEY WORDS: Crumbs, Galla, Xpd, Kinesin-5, Mitosis, Organ growth

INTRODUCTION

Crumbs (Crb) is a conserved transmembrane protein essential for epithelial apical–basal cell polarity in *Drosophila* (Tepass, 2012; Pocha and Knust, 2013; Martin-Belmonte and Perez-Moreno, 2012). Crb is also required for visual function in the eye by regulating apical morphogenesis of photoreceptor cell membranes (Hong et al., 2003; Izaddoost et al., 2002; Pellikka et al., 2002). In addition, Crb is involved in the regulation of Hippo signaling for organ growth (Chen et al., 2010; Ling et al., 2010; Ribeiro et al., 2014; Robinson et al., 2010). In these processes, Crb functions as an apical cue for interacting protein partners.

Recent evidence indicates that Crb is also required for controlling mitotic processes in *Drosophila* (Yeom et al., 2015). Segregation of chromosomes is a key process in mitosis that is coordinated by mitotic spindles. The *Drosophila* embryo has been extensively used to study mitosis *in vivo*. Embryogenesis in *Drosophila* begins with 13 cycles of nuclear division to generate a multinucleate syncytium prior to cellularization. Regulation of spindle microtubules is critical for precise chromosome segregation during these nuclear division cycles. A clue toward understanding the role of Crb in mitosis was provided by the genetic interaction of Crb with Galla-1 and Galla-2 (Yeom et al., 2015), two *Drosophila* homologs of mammalian MIP18 (also known as CIAO2B), a protein implicated in chromosome segregation (Ito et al., 2010). Crb and Galla proteins colocalize to the region of mitotic spindles during nuclear division in early embryos, and their loss results in various mitotic defects including branched/fused spindle microtubules and incomplete segregation of dividing nuclei (Yeom et al., 2015). Interestingly, MIP18 is known to bind XPD to form a protein complex (Ito et al., 2010). XPD (also known as ERCC2) is a DNA helicase that regulates DNA repair, the cell cycle and transcription by forming a complex with the TFIIH transcription factor. Mutations in XPD are associated with human diseases such as xeroderma pigmentosum, trichothiodystrophy and Cockayne syndrome (Egly and Coin, 2011; Zurita and Merino, 2003). MIP18 is not found in the TFIIH complex, but interacts with XPD to form a distinct protein complex called MMXD to regulate mitosis (Ito et al., 2010). It is unknown whether Galla proteins are independent from the TFIIH complex in *Drosophila*.

The *Drosophila* homolog Xpd is also required for mitosis during early embryogenesis (Chen et al., 2003; Li et al., 2010). Crb physically interacts with Galla and Xpd, and loss of these proteins results in mitotic defects with abnormal spindles (Yeom et al., 2015). Spindle microtubules are associated with various motor proteins (Hildebrandt and Hoyt, 2000; Mazumdar and Misteli, 2005; Goshima and Vale, 2003). Among these mitotic motors, Kinesin-5 plays a critical role in the formation and maintenance of bipolar spindles (Heck et al., 1993; Scholey, 2009). Kinesin-5 has a characteristic bipolar structure made of four monomeric motor proteins that allows sliding between two anti-parallel spindle microtubules (Acar et al., 2013; Kashina et al., 1996; Kapitein et al., 2005; Cole et al., 1994; Saunders et al., 2007). Such activity leads to the separation of two spindle poles from each other, resulting in the segregation of chromosomes (Kashina et al., 1997; Heck et al., 1993). *Drosophila* Klp61F is the ortholog of vertebrate Kinesin-5 family proteins and has both conserved structure and function (Vale and Milligan, 2000; Waitzman and Rice, 2014; Kashina et al., 1997; Heck et al., 1993). Although Crb–Galla–Xpd (CGX) proteins are known to have a role in mitosis, the details of how they are involved in the mitotic process remain a puzzle.

In this study, we demonstrate that the CGX proteins regulate mitosis by directly interacting with Klp61F kinesin. Depletion of Crb, Galla-2 or Xpd results in similar spindle defects. Genetic analysis suggests that Klp61F functions downstream of Galla-2 and Xpd. Loss of CGX proteins results in a proteasome-dependent reduction of Klp61F protein level. This work provides evidence that

Department of Biological Sciences, Korea Advanced Institute of Science and Technology, Daejeon 34141, Korea.
*Present address: Department of Developmental and Regenerative Biology and Graduate School of Biomedical Sciences, Icahn School of Medicine at Mount Sinai, New York, NY 10029, USA.
‡These authors contributed equally to this work

§Author for correspondence (kchoi100@kaist.ac.kr)

K.-W.C., 0000-0002-8997-3065

Handling Editor: David Glover
Received 25 March 2020; Accepted 29 April 2020

Journal of Cell Science (2020) 133, jcs246801. doi:10.1242/jcs.246801

CGX proteins are required to maintain the level of Klp61F protein for proper regulation of mitosis in the embryo. Our data also suggest important roles for Xpd and Klp61F in organ growth.

RESULTS

Identification of Klp61F as a genetic modifier of Crb

Overexpression of the intracellular domain of Crb (Crb^{intra}) in eye discs, driven by *GMR-Gal4*, causes severe roughening of adult eyes by affecting the integrity of the differentiating retinal epithelium (Izaddoost et al., 2002; Pellikka et al., 2002; Grzeschik and Knust, 2005) (Fig. 1D). Knockdown or overexpression of Klp61F by *GMR-Gal4* in the wild-type background did not alter the size or the morphology of adult eyes (Fig. 1A–C). However, this rough eye phenotype was strongly enhanced by knockdown of Klp61F (Fig. 1E) and suppressed by overexpression of Klp61F in all tested flies (Fig. 1F). As control, *GMR>crb^{intra}* was crossed with *UAS-GFP* to ensure that the suppression of Crb^{intra} by *UAS-Klp61F* was not due to titration of Gal4 by an additional copy of UAS (Fig. 1D).

Crb and Klp61F colocalize to mitotic spindles and physically interact

Genetic interaction between *crb* and *Klp61F* suggests that these two gene functions might be related in mitosis. Because analysis of mitosis in the eye disc is not straightforward due to the small cell size and unsynchronized mitosis, we chose to examine nuclear divisions in the syncytial embryo, which has been extensively utilized to study mitotic functions of Klp61F (Cheerambathur et al., 2008; Brust-Mascher et al., 2009; Scholey, 2009; Sharp et al., 1999). Embryos were examined at approximately nuclear division cycle 11, unless stated otherwise. Previously, we have shown that Crb is detected as diffused staining in the region of chromosome segregation during nuclear division (Yeom et al., 2015). We examined whether Crb localization showed any overlap with Klp61F in microtubule spindles during mitosis. Because we often found bleed-through effects from tubulin staining, we performed immunostaining for Crb and Klp61F in the absence of anti-tubulin antibody. In prophase, both Crb and Klp61F staining were enriched at the spindle poles (Fig. 2A) with a similar pattern to the tubulin staining (Fig. S1A). Although Crb staining appeared more diffuse than Klp61F staining, it showed a similar pattern with Klp61F and tubulin in mitotic spindles of metaphase (Fig. 2B; Fig. S1B) and anaphase (Fig. 2C; Fig. S1C). In telophase, tubulin was strongly localized to the midbody (Fig. S1D). Crb and Klp61F were also enriched in the region of the midbody (arrows in Fig. 2D). The specificity of anti-Crb staining in the syncytial embryo was demonstrated previously by loss of Crb staining after *crb RNAi* (Yeom et al., 2015). We also confirmed reduction of Klp61F levels in syncytial embryos produced from females treated with *Klp61F RNAi* using *maternal (mat)-Gal4* (Fig. S1E,F). These results suggest that the anti-Klp61F antibody and *Klp61F RNAi* work properly.

Based on their overlapping localization, we checked whether Crb and Klp61F physically interact. In an assay using S2 cells transfected with Myc–Crb^{intra} and Flag–Klp61F, Flag–Klp61F co-immunoprecipitated with Myc–Crb^{intra}. However, a negative control Kinesin II subunit Klp64D, which shares a conserved motor domain with Klp61F (41% sequence identity), was not co-immunoprecipitated with Crb (Fig. 2E). We also performed pulldown experiments using bacterially expressed GST-fusion proteins. GST–Crb^{intra} could bind to Klp61F but not Klp64D (Fig. 2F), indicating their specific interaction.

Klp61F suppresses mitotic defects that result from Crb^{intra} overexpression

To examine the functional relationship between Crb and Klp61F, we compared mitotic defects caused by Crb^{intra} overexpression and *Klp61F RNAi.* Because loss-of-function mutations in *crb* or *Klp61F* cause lethality, we examined the effects of RNAi knockdown in the germline of mothers using *mat-Gal4*. As reported previously (Garcia et al., 2009; Heck et al., 1993; Wilson et al., 1997), Klp61F knockdown by RNAi (*Klp61F RNAi^{BL35804}*) caused spindle defects in different phases of cortical nuclear division. Similar mitotic defects were seen in an independent RNAi line (*Klp61F RNAi^{V52548}*) (Fig. S2A,B). Examination of embryos at cycle 11 indicated that most embryos (79%) showing mitotic defects were in metaphase (Fig. S2I,J,L). Likewise, a majority of embryos (69%) with Crb^{intra} overexpression showed spindle defects during metaphase (Fig. S2I,K,L), similar to *crb RNAi* phenotypes (Fig. S2G,H). Therefore, we focused our analysis on mitotic defects during metaphase at cycle 11. There were three major common types of spindle defects caused by overexpression of Crb^{intra} or *Klp61F RNAi*: free centrosomes with no attached spindles and chromosomes, fused/branched microtubules, and multiple poles and monopolar spindles (Fig. 3A–C; Fig. S6). The most frequent phenotype of Crb^{intra} overexpression was free centrosomes, compared to lower incidence of multi-polar and monopolar phenotypes. Spindle phenotypes resulting from Crb^{intra} overexpression were considerably recovered by Klp61F overexpression (Fig. 3G).

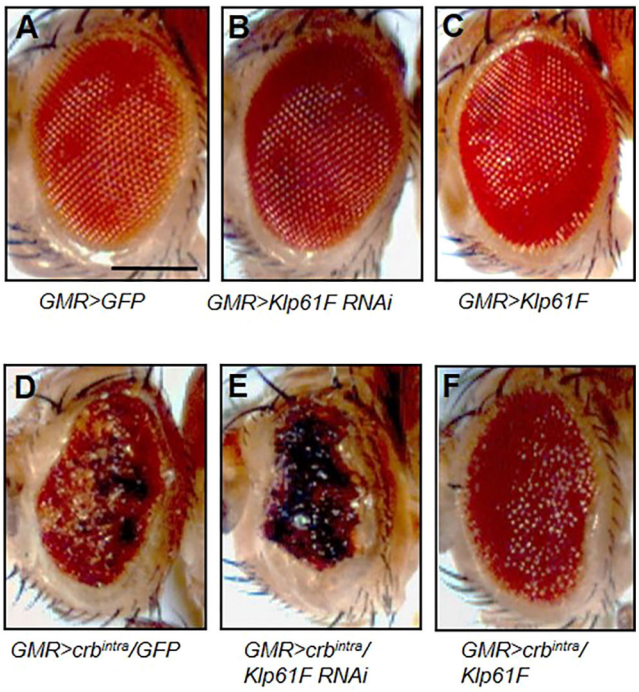

Fig. 1. Genetic interaction between *crb* and *Klp61F*. (A–F) Genetic interaction between *crb* and *Klp61F* in the eye. Scale bar: 200 µm. (A) *GMR-Gal4* crossed with *UAS-GFP* as a control. (B) Knockdown of Klp61F and (C) Klp61F overexpression show normal eyes. (D) Overexpression of Crb^{intra} under *GMR-Gal4* results in a rough eye phenotype. (E) *Klp61F RNAi* enhances the Crb^{intra} phenotype, resulting in smaller eyes with severely rough and blackened ommatidia (100%, *n*=44). (F) Overexpression of Klp61F partially suppresses the Crb^{intra} phenotype, showing enlarged eyes with reduced roughness (100%, *n*=52).

Journal of Cell Science (2020) 133, jcs246801. doi:10.1242/jcs.246801

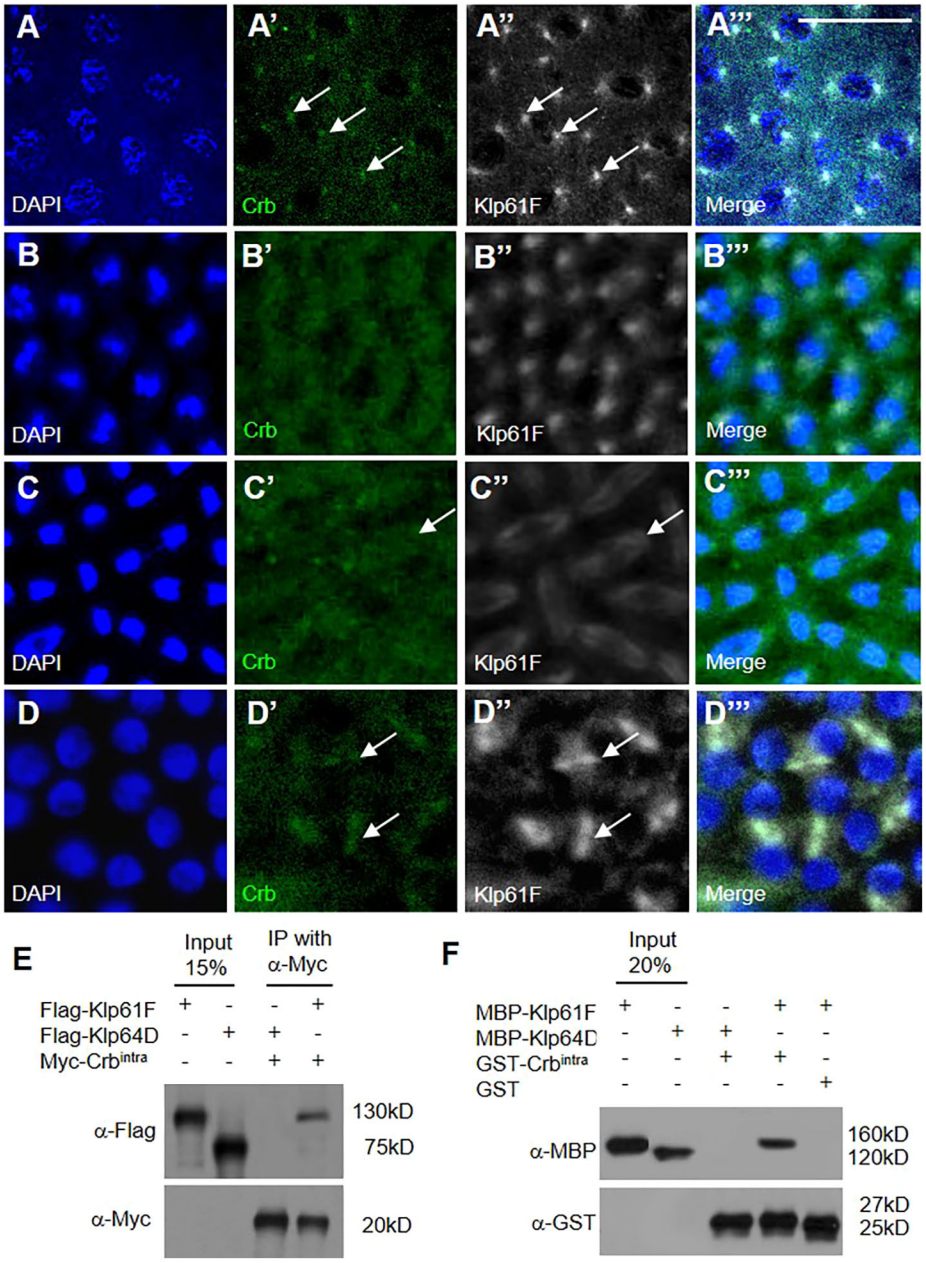

Fig. 2. Localization and physical interaction of Crb and Klp61F. (A–D‴) Localization of Crb and Klp61F during nuclear division in syncytial embryos. Nuclei are stained with DAPI. Scale bar: 20 µm. (A) Both Crb and Klp61F are enriched in spindle poles during prophase (arrows in A′ and A″). (B,C) Crb and Klp61F show similar spindle staining during metaphase (B) and anaphase (C). Crb shows a diffused pattern that partially overlaps with Klp61F (arrows in C′ and C″). (D) Klp61F is localized to the midbody, and Crb is also enriched in the midbody during telophase (arrows in D′ and D″). (E) Co-immunoprecipitation of Klp61F and Crb. *Drosophila* S2 cells were transfected with Flag–Klp64D (lane 3) or Flag–Klp61F (lane 4) and Myc-Crb^{intra}. Lane 1 and 2 are loaded with 15% of input for Flag–Klp61F and Flag–Klp64D, respectively. Anti-Myc was used for IP, and Myc–Crb^{intra} co-immunoprecipitated Flag–Klp61F but not Flag–Klp64D. Molecular masses in kDa (kD) are shown. (F) Direct binding between Klp61F and Crb. Lane 1 and 2 show 20% input for MBP–Klp61F and MBP–Klp64D, respectively. GST–Crb^{intra} pulled down Klp61F but not Klp64D. Molecular masses in kDa (kD) are shown.

After the ninth nuclear division cycle, most nuclei migrate to the periphery of the embryo to form a monolayer at the cortex prior to cellularization (Mazumdar and Mazumdar, 2002; Foe and Alberts, 1983). *Klp61F RNAi* and Crb^{intra} overexpression often led to loss of nuclei in large patches where multiple mitotic nuclei fell into the interior of the embryo. Such nuclei-free patches were found at a low frequency during nuclear division cycle 10. However, the frequency of nuclei-free patches was significantly increased later in nuclear division cycles 12–13. Because the type of spindle defects could not be determined in such regions of nuclear loss, we scored such phenotype separately based on the severity of nuclear loss. We divided the nuclear-loss phenotypes into ‘mild’ and ‘severe’ phenotypes which refer to embryos showing less than 10% or more than 10% of nuclei-free area, respectively (Fig. 3D–F). In wild-type controls, ∼75% of embryos were normal whereas 10–15% embryos showed mild or severe nuclear-loss phenotype. Crb^{intra} overexpression resulted in the nuclear-loss phenotype in ∼85% of embryos, and these phenotypes were partially suppressed by overexpressing Klp61F (Fig. 3H). Thus, Klp61F overexpression can suppress Crb^{intra} phenotypes not only in the eye but also in mitosis during early embryogenesis.

Galla-2 knockdown is suppressed by Klp61F overexpression

Galla-1 and Galla-2 are related *Drosophila* homologs of mammalian MIP18, a protein associated with XPD (Ito et al., 2010). Because Galla proteins interact with Crb^{intra} (Yeom et al., 2015), we tested whether Galla-1 and/or Galla-2 might also be associated with Klp61F. Both V5–Galla-1 and V5–Galla-2 expressed in S2 cells were co-immunoprecipitated with Flag–Klp61F, whereas Galla-1 was not co-immunoprecipitated with Flag–Klp64D negative control (Fig. 4A). Endogenous Galla-2 and Klp61F proteins were also co-immunoprecipitated in tissue extracts from wild-type embryos or adult heads (Fig. S3A), suggesting these proteins form a complex *in vivo*. In GST

Journal of Cell Science (2020) 133, jcs246801. doi:10.1242/jcs.246801

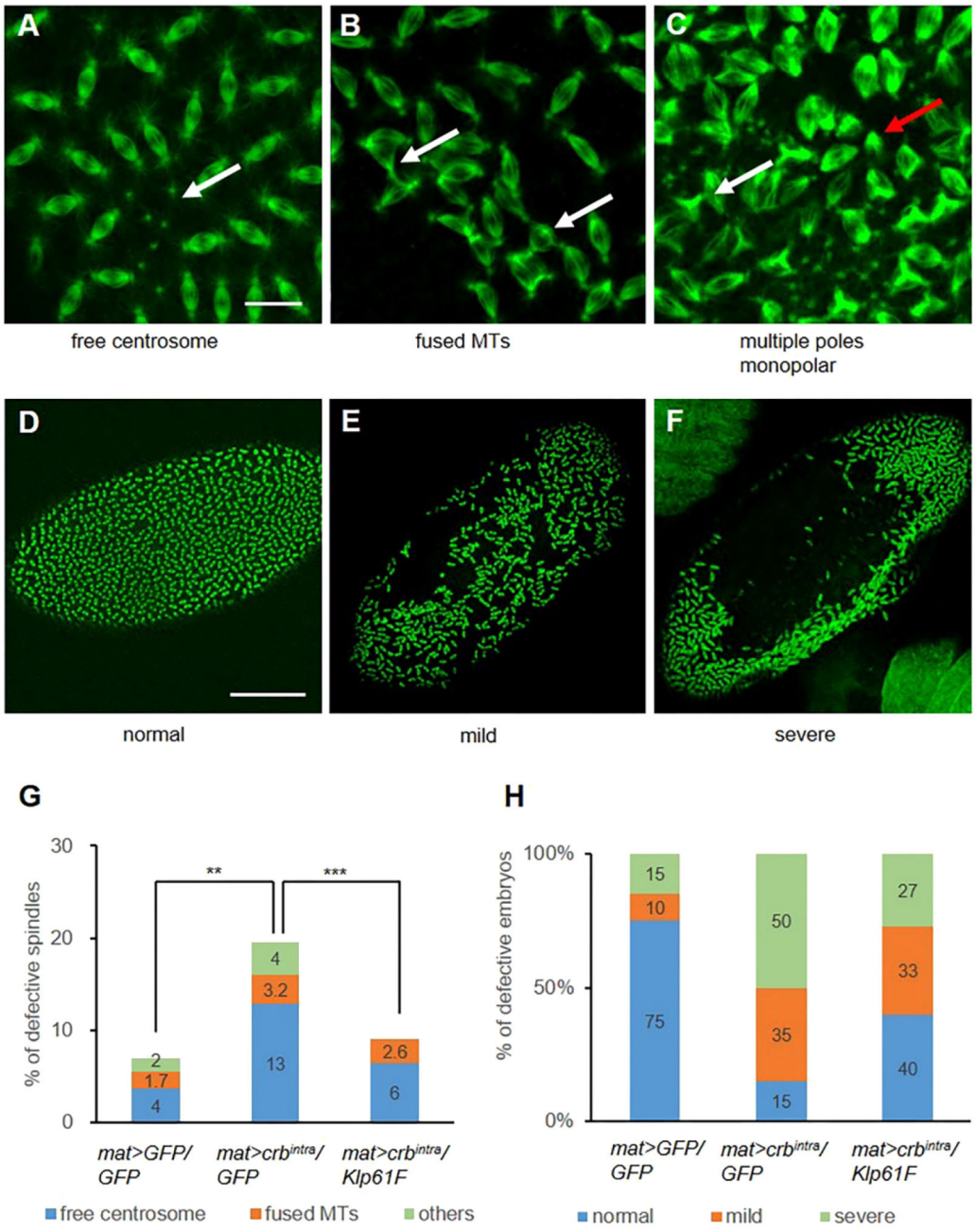

Fig. 3. Spindle defects and nuclear loss caused by Crb^{intra} overexpression are suppressed by Klp61F overexpression. (A–C) Spindle defects caused by Crb^{intra} overexpression. Spindles are labeled with anti-tubulin antibody. (A) Free centrosomes that are not associated with spindles and chromosomes (arrow). (B) Fusion of spindles from two adjacent nuclei (arrows). (C) Multiple poles (white arrow) or monopolar spindles (red arrow). (D–F) Nuclear loss phenotype, as assayed by tubulin staining, is divided into three categories: normal (D), mild (less than 10% loss; E) and severe (more than 10% loss; F). (G) Quantification of spindle defects. The spindle phenotypes are suppressed by Klp61F overexpression. Statistical significance was tested for combined defective spindle phenotypes. *n*>26. ***P*<0.01, ****P*<0.001. Results of *t*-tests for each phenotype are shown in Table S1. (H) Quantification of nuclear-loss phenotypes. Klp61F overexpression partially suppresses Crb^{intra} overexpression phenotypes. *n*>80. Scale bars: 20 µm for A–C, 100 µm for D–F.

pulldown assays, GST–Galla-2 showed direct binding to Klp61F but not Klp64D. Interestingly, GST–Galla-1 did not show detectable binding to Klp61F (Fig. 4B). Hence, Galla-2 directly interacts with Klp61F, whereas Galla-1 might associate with Klp61F indirectly.

Consistent with the physical interaction between Galla-2 and Klp61F, immunostaining of Galla-2 in the absence of anti-tubulin antibody showed localization of Galla-2 to spindles (Fig. 4C), in the same pattern as tubulin staining (Fig. S3B). Maternal knockdown of Galla-2 strongly reduced Galla-2 levels in the spindles of dividing nuclei (Fig. S3C), supporting the specificity of Galla-2 staining and *galla-2 RNAi*. We then examined the effects of Galla-2 knockdown in mitotic nuclei in early embryos. Maternal knockdown of Galla-2 by two independent RNAi lines (v110611 and BL58320) showed similar types of mitotic spindle defects, such as free centrosomes and fused spindles (Figs S2C,D and S6), as seen with Crb^{intra} overexpression. These *galla-2 RNAi* defects were strongly suppressed by Klp61F overexpression, reducing from 27% to 3.2% of spindles (Fig. 4D). A high level of severe nuclear

Journal of Cell Science (2020) 133, jcs246801. doi:10.1242/jcs.246801

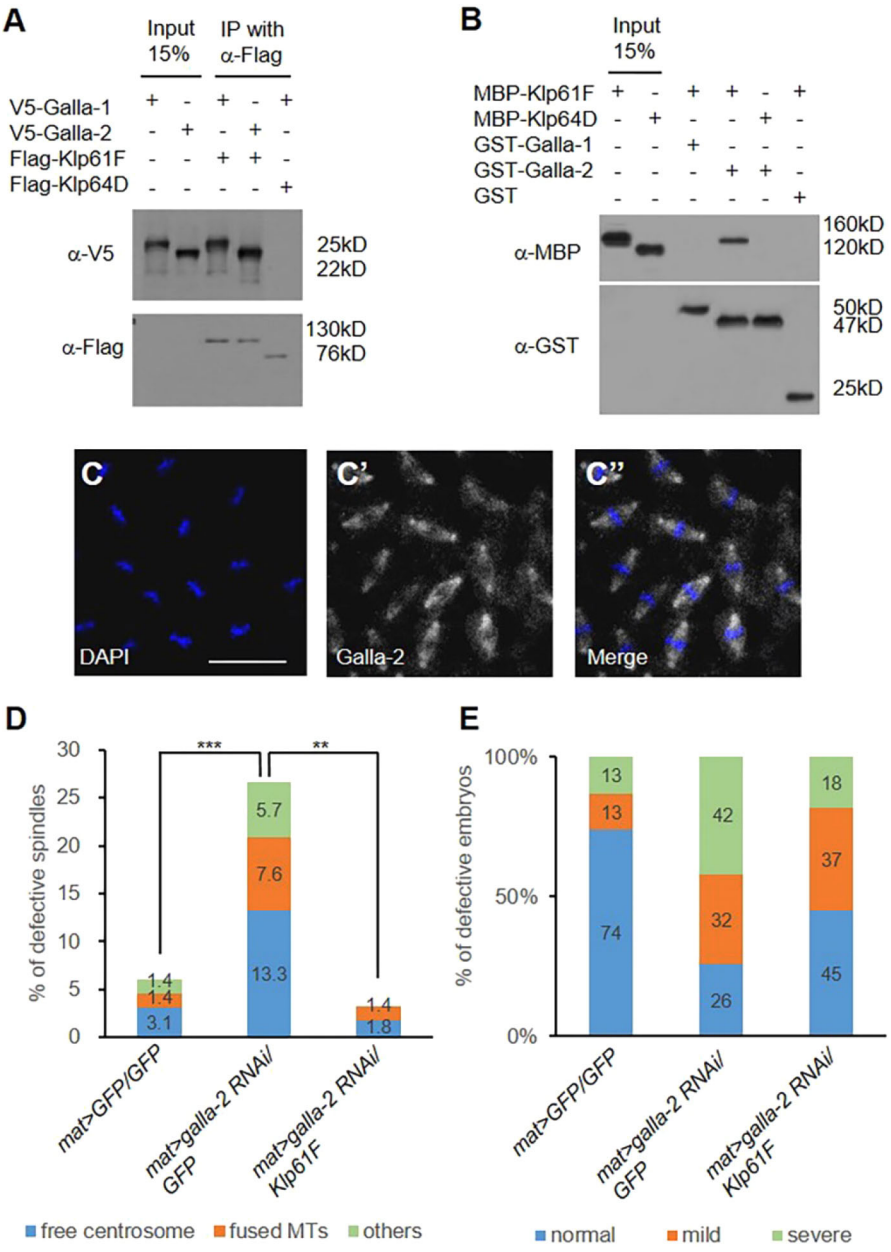

Fig. 4. Genetic and physical interaction between Klp61F and Galla. (A) S2 cells were transfected with Flag–Klp61F, Flag–Klp64D, V5–Galla-1 and V5–Galla-2. Lanes 1 and 2 are loaded with 15% of input of V5–Galla-1 and V5–Galla-2, respectively. Anti-Flag antibody was used for IP, and both Galla-1 and Galla-2 were co-immunoprecipitated with Klp61F (lanes 3 and 4). Galla-1 was not co-immunoprecipitated with Klp64D (lane 5). Molecular masses in kDa (kD) are shown. (B) Direct binding between Klp61F and Galla. Lanes 1 and 2 are 15% input of MBP–Klp61F and MBP–Klp64D, respectively. Klp61F was pulled down by GST–Galla-1 (lane 3) and GST–Galla-2 (lane 4). GST–Galla-2 did not pull down Klp64D (lane 5). Only Galla-2 shows direct interaction with Klp61F. Molecular masses in kDa (kD) are shown. (C–C″) Galla-2 shows localization to spindles in syncytial embryos. Nuclei are stained with DAPI. Scale bar: 20 µm. (D) Quantification of spindle defects caused by *galla-2 RNAi*, scored as described in Fig. 3. Spindle defects are suppressed by Klp61F. $n>24$. Statistical significance was tested for combined defective spindle phenotypes. $^{**}P<0.01$, $^{***}P<0.001$. Results of *t*-tests for each phenotype are shown in Table S1. (E) Quantification of nuclear-loss phenotypes, scored as described in Fig. 3. $n>75$. Klp61F overexpression partially suppresses *galla-2 RNAi* phenotypes.

loss (42% of embryos) also resulted from *galla-2 RNAi*. The nuclear-loss phenotype was partially suppressed to 18% by Klp61F overexpression (Fig. 4E).

Xpd RNAi phenotypes are suppressed by Klp61F overexpression

Galla-2 physically interacts with Xpd (Yeom et al., 2015). We also found that Myc–Xpd colocalizes with GFP–Klp61F in mitotic spindles of dividing S2 cells (Fig. S1G). Hence, Xpd might function together with Klp61F in mitosis. Immunoprecipitation assays indicated that Myc–Xpd forms a complex with Flag–Klp61F in S2 cells (Fig. 5A). Furthermore, GST-pulldown assays showed direct binding between MBP–Klp61F and GST–Xpd protein (Fig. 5B). In these interaction assays, Xpd did not show physical interaction with the negative control Klp64D in co-immunoprecipitation or GST-pulldown tests (Fig. 5A,B).

Xpd knockdown by *mat-Gal4* using two *Xpd RNAi* lines (v106998 and v41021) led to similar spindle defects in early embryos (Figs S2E,F and S6). The majority of the observed spindle defects were free centrosomes. Spindle defects caused by *Xpd RNAi* were restored to the level of control (*mat>GFP/GFP*) by overexpressing Klp61F (Fig. 5C). As in *galla-2*-depleted embryos, *Xpd RNAi* resulted in large regions of nuclear loss in early embryos. The nuclear-loss phenotype was also weakly suppressed by Klp61F overexpression (Fig. 5D). Although Klp61F overexpression did not change the level of total defective embryos (77% of embryos without Klp61F overexpression compared to 75% of embryos with overexpression), it significantly reduced the number of severely defective embryos (from 60% to 41%). Taken together, mitotic defects caused by *Xpd RNAi* can be partially compensated by Klp61F overexpression.

Knockdown of Crb, Galla-2 or Xpd causes a proteasome-dependent reduction in Klp61F levels

Because mitotic defects from Crb^{intra} overexpression or knockdown of CGX genes can be suppressed by Klp61F overexpression, these

Journal of Cell Science (2020) 133, jcs246801. doi:10.1242/jcs.246801

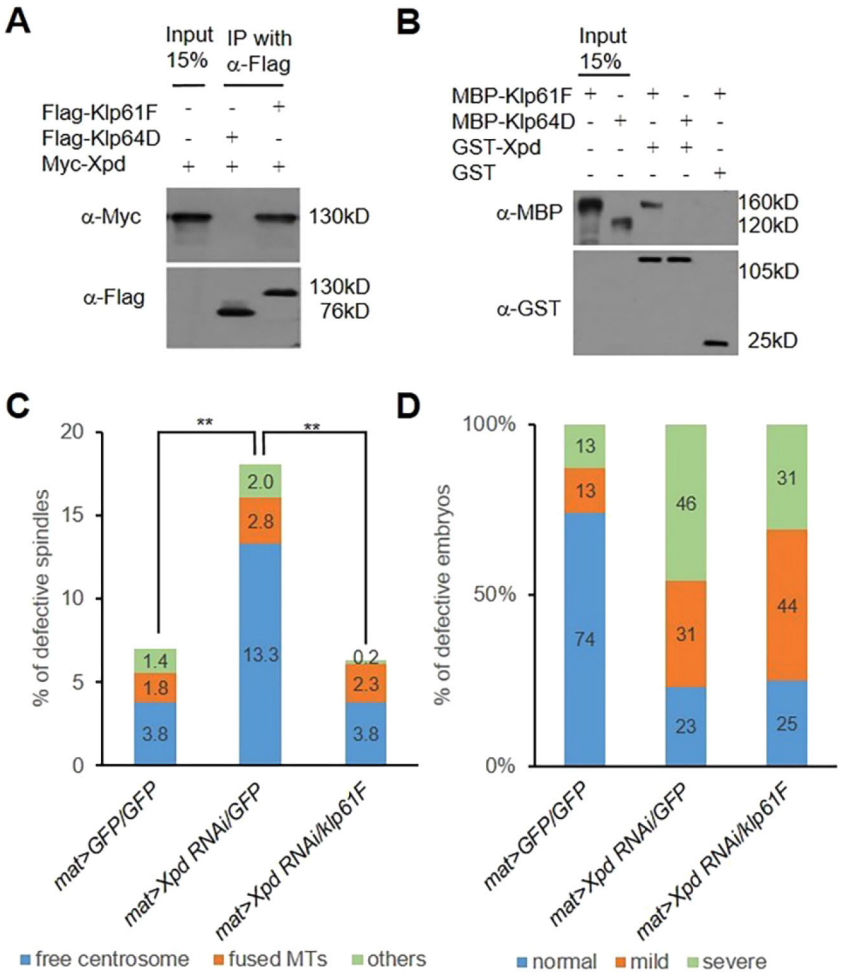

Fig. 5. Genetic and physical interaction between Klp61F and Xpd. (A) Co-immunoprecipitation of Klp61F and Xpd from S2 cells transfected with Flag–Klp64D (lane 2) or Flag-Klp61F (lane 3) and Myc–Xpd. Lane 1 is 15% input of Myc–Xpd. Myc–Xpd is co-immunoprecipitated with Flag–Klp61F but not with Flag–Klp64D. Molecular masses in kDa (kD) are shown. (B) Direct binding of Klp61F and Xpd. Lanes 1 and 2 are 15% input of MBP–Klp61F and MBP–Klp64D, respectively. Klp61F was pulled down by GST–Xpd (lane 3) but not by GST (lane 5). Klp64D shows no interaction with GST–Xpd (lane 4). Molecular masses in kDa (kD) are shown. (C) Quantification of spindle defects caused by *Xpd RNAi* and their suppression by Klp61F, scored as described in Fig. 3. $n>24$. Statistical significance was tested for combined defective spindle phenotypes. $^{**}P<0.01$. Results of *t*-tests for each phenotype are shown in Table S1. (D) Quantification of nuclear loss by *Xpd RNAi* and its suppression by Klp61F, scored as described in Fig. 3. $n>84$.

genes might be involved in the regulation of Klp61F protein levels. To test this possibility, first we attempted to examine Klp61F levels by western blotting. Tissue extracts were prepared from syncytial embryos collected over a 2 h period. Western blotting revealed that Klp61F levels were variably reduced by knockdown of Crb, Galla-2 or Xpd, and by Crb^{intra} overexpression. The variable reductions were probably due to heterogeneity in the severity of nuclear loss of the collected embryos. Quantitative data from 20 western blot experiments showed that maternal knockdown of Crb, Galla and Xpd resulted in an ∼55% reduction in the relative Klp61F level, normalized to tubulin levels. Overexpression of Crb^{intra} also showed similar levels of Klp61F reduction (Fig. S5A, Table S2). Because western blot results can be affected by variable degrees of nuclear loss, we also checked the level of Klp61F in mitotic spindles of syncytial embryos. Compared with *mat>GFP* control embryos (Fig. 6A), embryos with maternal overexpression of Crb^{intra} showed reduced levels of Klp61F in anaphase spindles (Fig. 6B). Similarly, knockdown of Galla-2 or Xpd significantly decreased the level of Klp61F staining (Fig. 6C,D). These data suggest that the CGX proteins are important for the maintenance of Klp61F during nuclear division.

Our results above raised a possibility that Klp61F may be downregulated in CGX-depleted embryos by proteasome-dependent degradation. Hence, we examined whether relative Klp61F levels, normalized to tubulin, can be recovered by partially impairing proteasome function. For partial loss of proteasome function, we utilized a mutation in *Rpt5*, a regulatory subunit of the proteasome complex. As shown in Fig. S5B, Crb^{intra} overexpression or knockdown of Galla-2 reduced the level of Klp61F. However, $Rpt5^{04210b}$/+ heterozygous mutation resulted in considerable elevation of Klp61F levels (Fig. S5B). Similarly, knockdown effects of *Klp61F RNAi* were suppressed by $Rpt5^{04210b}$/+, thus increasing the Klp61F level (Fig. S5B). Quantification of 20 western blot assays showed that reduced Klp61F levels caused by Crb^{intra} overexpression, *galla-2 RNAi* or *Klp61F RNAi* were significantly increased by $Rpt5^{04210b}$/+ to 1.4–1.8-fold higher levels than the control (*mat>GFP/GFP*) level (Fig. S5B, Table S3).

Next, we asked whether mitotic defects of *galla-2 RNAi* can be suppressed by reducing proteasome function. Spindle defects caused by *galla-2 RNAi* were strongly suppressed by the $Rpt5^{04210b}$/+ heterozygous mutant condition (Fig. 7A,C). $Rpt5^{04210b}$/+ heterozygosity also suppressed mitotic defects of *Klp61F RNAi* (Fig. 7A,D), consistent with the recovery of Klp61F levels (Fig. S5B, Table S3). We also examined the effects of mutation in a different proteasome component Prosβ6. Mitotic defects from *galla-2 RNAi* or Crb^{intra} overexpression were strongly suppressed by $Pros\beta6^{1}$/+ heterozygous condition (Fig. 7B,E,F).

galla-2 RNAi defects are suppressed by Xpd, but not vice versa

As shown earlier, mitotic defects of *galla-2 RNAi* and *Xpd RNAi* are suppressed by overexpression of Klp61F (Figs 4, 5), suggesting that Klp61F might act downstream of Galla-2 and Xpd. However, the functional relationship between Galla-2 and Xpd has not been

Journal of Cell Science (2020) 133, jcs246801. doi:10.1242/jcs.246801

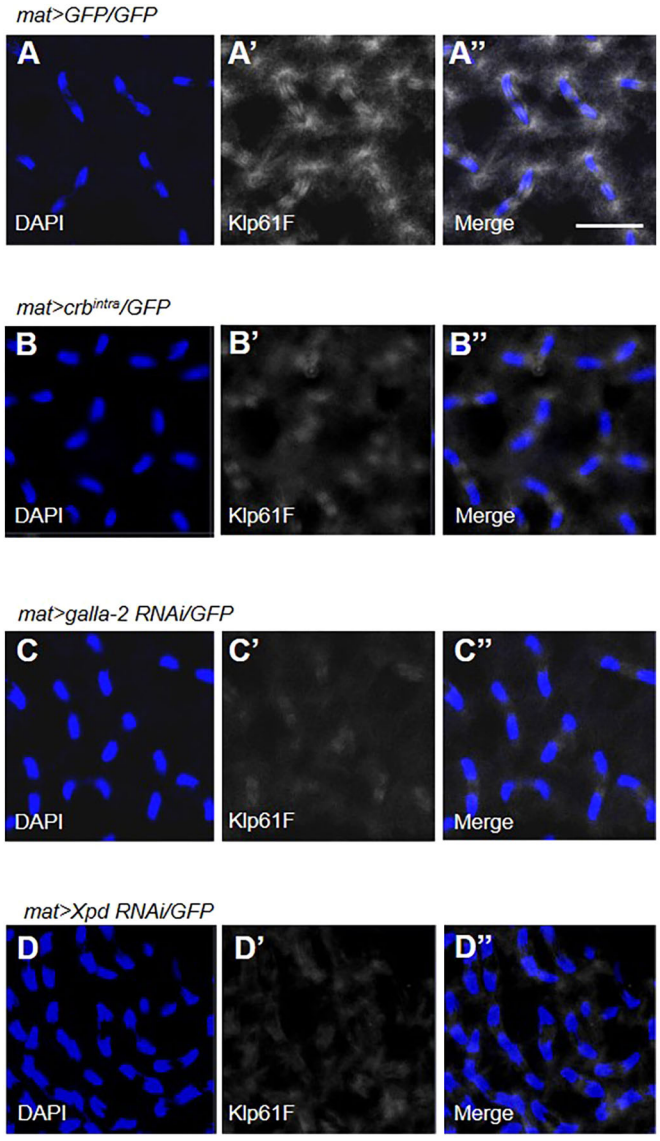

Fig. 6. Klp61F levels are reduced by Crb^{intra} overexpression and by *galla-2* or *Xpd RNAi*. (A–A″) In *mat>GFP/GFP* control embryos, Klp61F localization shows the pattern of mitotic spindles in anaphase of nuclear division. (B–B″) Crb^{intra} overexpression using *mat-Gal4* results in reduced levels of Klp61F. (C–D″) Effects of maternal knockdown of Galla-2 and Xpd. Klp61F levels were reduced by *galla-2 RNAi* (C) or *Xpd RNAi* (D). Scale bar: 20 µm. DAPI staining of nuclei is shown in blue, Klp61F staining is shown in white.

tested. Interestingly, we noted that Galla-2 levels were strongly reduced in mitotic nuclei of *Xpd RNAi* embryos (Fig. S4C). However, Galla-2 overexpression had little restorative effect on the spindle defects resulting from *Xpd RNAi* (Fig. 8A). Conversely, Xpd overexpression strongly suppressed spindle defects caused by *galla-2 RNAi* (Fig. 8B). Hence, although Galla-2 protein levels are affected by Xpd, Galla-2 function in mitosis depends on Xpd, but not vice versa.

Because we found a genetic interaction between Crb and Klp61F in the eye (Fig. 1), we tested whether Xpd and Klp61F have a similar functional relationship in eye development. *Xpd RNAi* using *ey-Gal4* resulted in significant reduction of the eye size compared to control eyes (Fig. 8C,G). This eye phenotype was fully rescued by Xpd overexpression, suggesting a specific effect of *Xpd RNAi* (Fig. 8G,H). In contrast, Galla-2 overexpression or *galla-2 RNAi* did not show any noticeable defects in adult eyes (Fig. 8E,F). Thus, Galla-2 is essential for nuclear division in embryos but may be dispensable for development of the adult eye. Due to the lack of an eye phenotype for *galla-2 RNAi*, we could not test whether Xpd overexpression can suppress the *galla-2 RNAi* phenotype, as in embryos (Fig. 8B). However, using the *Xpd RNAi* eye phenotype, we asked whether Galla-2 overexpression can suppress the *Xpd RNAi* eye defects. In this test, Galla-2 overexpression failed to suppress the *Xpd RNAi* eye phenotype (Fig. 8J), consistent with the relationship in embryos (Fig. 8A).

We then checked whether the eye phenotype resulting from *Xpd RNAi* can be ameliorated by overexpression of Klp61F. Although Klp61F overexpression did not affect eye growth in the normal condition (Fig. 8D), it strongly suppressed the *Xpd RNAi* eye phenotype (Fig. 8I), consistent with the suppression of mitotic phenotype of *Xpd RNAi* by Klp61F overexpression in embryos. These data suggest that Klp61F overexpression can bypass the defects of Xpd in two distinct developmental contexts, mitosis in the syncytial embryo and eye growth.

DISCUSSION

Mitotic segregation of chromosomes is crucial for genome stability in all eukaryotes. Kinesin-5-family mitotic motor proteins play a key role in formation of bipolar spindles necessary for chromosome segregation during mitosis. In this study, we have provided evidence that Crb, Galla-2 and Xpd proteins regulate Klp61F for proper chromosome segregation during nuclear division in early embryogenesis.

Crb, Galla-2 and Xpd regulate Klp61F levels

Crb, Galla-2 and Xpd proteins were enriched in mitotic spindles and showed physical interaction. Syncytial embryos with reduced function of Crb, Galla-2, or Xpd had similar defects in mitotic spindles. These mitotic defects could be suppressed by maternal overexpression of Klp61F, indicating that Crb, Galla-2 and Xpd are required for the function of Klp61F in mitosis. Our data lead us to propose that CGX proteins are required for the maintenance of bipolar spindles where they regulate the level of Klp61F in a proteasome-dependent manner. This idea is supported by two observations: firstly, Klp61F protein levels were restored by reducing the function of proteasome subunits. Secondly, mitotic defects resulting from knockdown of Galla-2 or Klp61F could also be recovered by reducing proteasome function.

Interestingly, it has been reported that Crb interacts with and stabilizes Myosin V, a motor protein, to regulate rhodopsin transport during retinal differentiation (Pocha et al., 2011). Hence, it could be possible that Crb, together with Galla and Xpd, is involved in regulating the stability of multiple proteins in diverse cellular processes. An alternative possibility is that CGX proteins might be involved in the regulation of Klp61F synthesis. In this case, proteasome-dependent degradation might facilitate the depletion of Klp61F in the context of impaired Klp61F synthesis. Under this condition, inhibition of the proteasome function might help maintain Klp61F levels for a limited time.

Physical interaction of CGX proteins with Klp61F raises the possibility that CGX might be required for stable association of Klp61F with spindles. This possibility is consistent with the results that *galla-2* or *Xpd RNAi* significantly reduced the level of Klp61F on spindles (Fig. 6). Furthermore, overexpression of Klp61F was sufficient to overcome mitotic defects caused by impaired CGX protein function (Figs 3–5). This suggests that overexpressed

Journal of Cell Science (2020) 133, jcs246801. doi:10.1242/jcs.246801

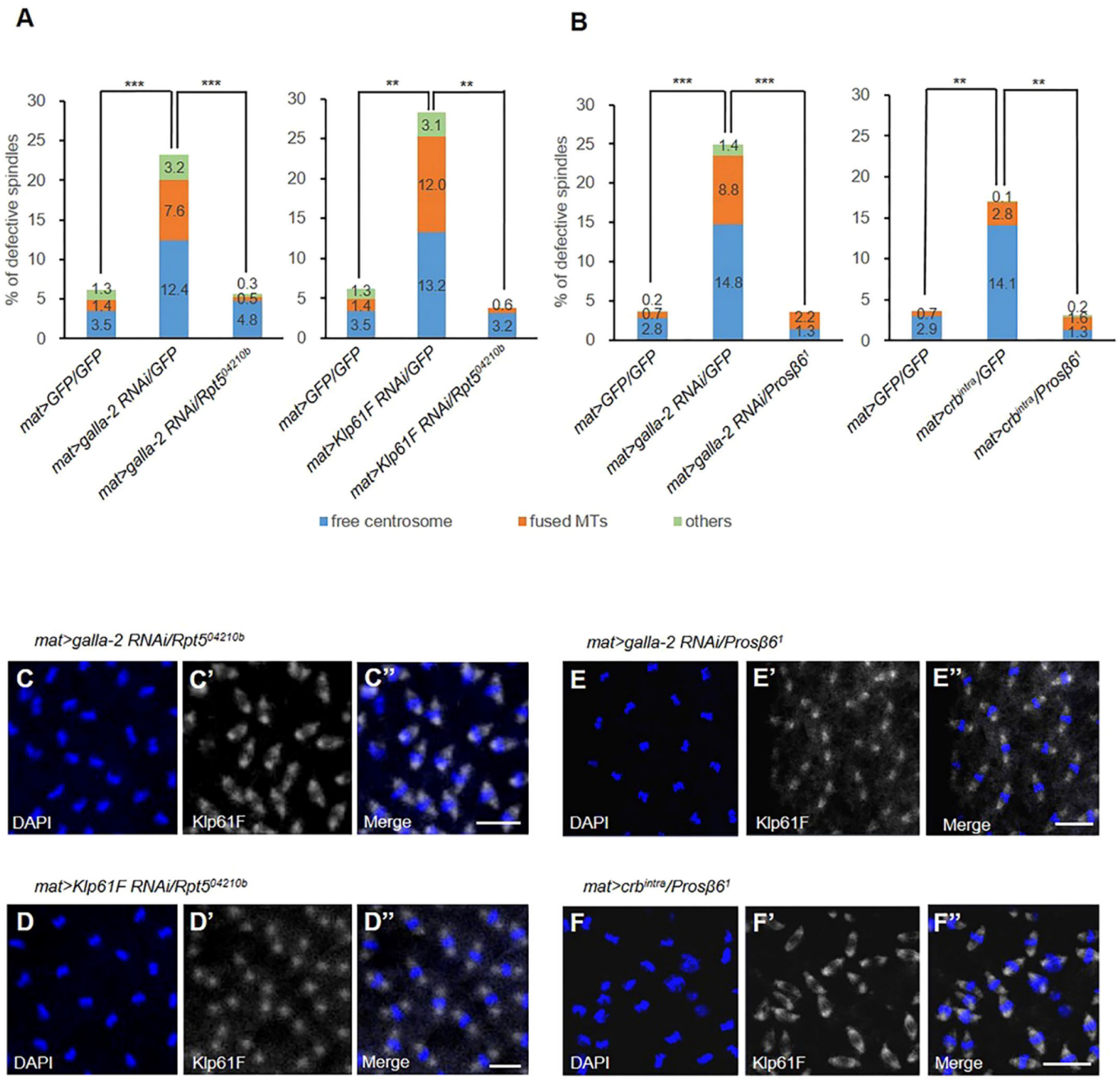

Fig. 7. Crb, Galla and Xpd are required for Klp61F stability. (A) Effects of *Rpt5*^{04210b}/+ heterozygous mutation. *Rpt5*^{04210b}/+ heterozygous mutation can suppress spindle defects caused by *galla-2 RNAi* or *Klp61F RNAi*, scored as described in Fig. 3. Statistical significance was tested for combined defective spindle phenotypes. *n*>16. ***P*<0.01, ****P*<0.001. Results of *t*-tests for each phenotype are shown in Table S1. (B) Effects of *Prosβ6*^{1}/+ heterozygous mutation on spindle defects. Spindle defects from *galla-2 RNAi* or Crb^{intra} overexpression are restored by *Prosβ6*^{1}/+ heterozygous mutation. *n*>17. Statistical significance was tested for combined defective spindle phenotypes. ***P*<0.01, ****P*<0.001. Results of *t*-tests for each phenotype are shown in Table S1. (C–F″) Effects of *Rpt5*^{04210b}/+ and *Prosβ6*^{1}/+ heterozygous mutations on Klp61F level. *Rpt5*^{04210b}/+ suppresses mitotic defects of maternal knockdown of Galla-2 (C–C″) or Klp61F (D–D″). *Prosβ6*^{1}/+ suppresses mitotic defects of maternal knockdown of Galla-2 (E–E″) or of Crb^{intra} overexpression (F–F″). Phenotypes of *galla-2 RNAi*, *Klp61F RNAi* and Crb^{intra} overexpression are shown in Fig. S2. Nuclei are stained with DAPI (blue, C–F), Klp61F staining is shown in white (C′–F′). Scale bar: 20 µm.

Klp61F proteins are functional even under the CGX RNAi condition. If CGX proteins are required to activate the function of Klp61F, overexpressed Klp61F alone would be insufficient to suppress CGX RNAi phenotypes. Therefore, CGX proteins might be required to stabilize Klp61F protein rather than to promote its activity. However, because we analyzed the effects of Klp61F overexpression following partial knockdown of CGX genes, we cannot exclude the possibility that residual CGX proteins might be able to promote the activity of overexpressed Klp61F. Studies with maternal null conditions for CGX proteins might help understand the function of the physical interaction of these proteins with Klp61F.

Galla-2 is required for Xpd function, but not vice versa

Galla-1 and Galla-2 are related homologs of mammalian MIP18. MIP18 is part of the MMXD complex involved in chromosome

Journal of Cell Science (2020) 133, jcs246801. doi:10.1242/jcs.246801

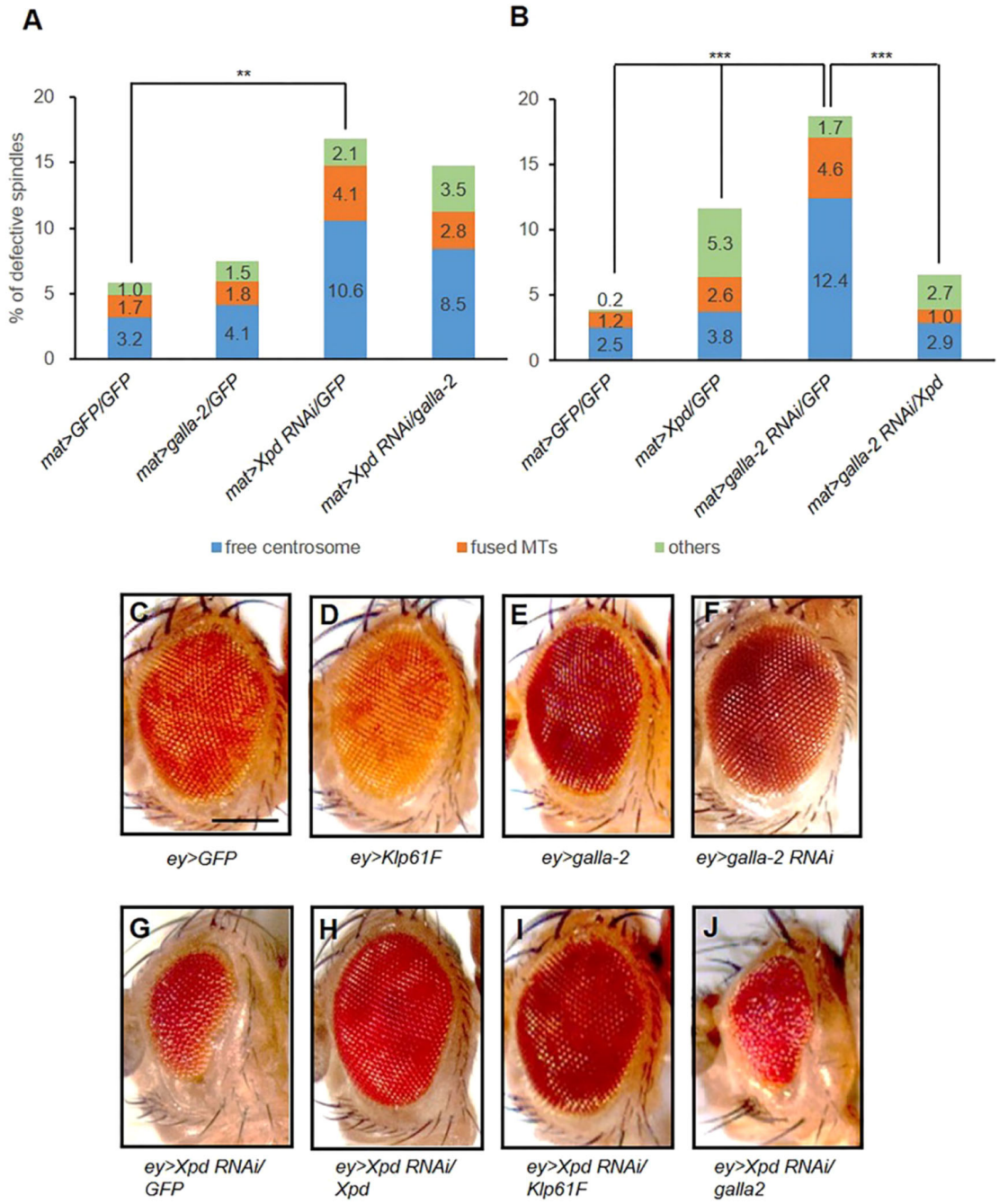

Fig. 8. *Xpd RNAi* phenotypes are suppressed by overexpression of Klp61F but not by Galla-2. (A) Galla-2 overexpression using *mat-Gal4* has no significant effect in the embryo. Spindle defects, scored as described in Fig. 3, resulting from *Xpd RNAi* are not significantly recovered by Galla-2 overexpression. Statistical significance was tested for combined defective spindle phenotypes. *n*=27. ***P*<0.01. Results of *t*-tests for each phenotype are shown in Table S1. (B) Spindle defects caused by *galla-2 RNAi* are rescued by Xpd overexpression. Note that overexpression of Xpd using *mat-Gal4* causes spindle defects in embryos. Spindle defects were scored as described in Fig. 3. Statistical significance was tested for combined defective spindle phenotypes. *n*=26. ****P*<0.001. Results of *t*-tests for each phenotype are shown in Table S1. (C–I) Adult eye phenotypes. *ey>GFP* control (C), overexpression of Klp61F (D), Galla-2 overexpression (E) and *galla-2 RNAi* (F) show normal eyes. (G) Knockdown of Xpd under *ey-Gal4* (*ey>Xpd RNAi*) shows a small-eye phenotype. (H) The small-eye phenotype of *Xpd RNAi* is rescued by Xpd overexpression (*n*=31). (I) Overexpression of *Klp61F* suppresses the small-eye phenotype caused by *Xpd RNAi* (*n*=32). (J) Overexpression of Galla-2 cannot rescue the small-eye phenotype of *Xpd RNAi* (*n*=30). Scale bar: 200 µm.

segregation (Ito et al., 2010), but its functional relationship with XPD is not well understood. Despite their sequence similarity, XPD preferentially binds to Galla-2 (Yeom et al., 2015), consistent with the strong genetic interaction seen between Galla-2 and Xpd. In embryonic nuclear division, *galla-2 RNAi* phenotypes could be suppressed by Xpd overexpression, but *Xpd RNAi* phenotypes could not be restored by Galla-2 overexpression (Fig. 8A,J). This indicates that Galla-2 is required for the function of Xpd in syncytial embryos, but not vice versa. However, Galla-2 levels in mitotic spindles were also reduced by knockdown of Xpd or Klp61F (Fig. S4). Therefore, although Galla-2 seems to act upstream of Xpd and Klp61F, its levels are influenced by downstream factors. A recent study has

shown that *Drosophila* Mms19, a Galla partner, binds to Xpd to release the Cdk-activating kinase (CAK) complex, thus activating Cdk1 for mitotic progression (Nag et al., 2018). Because Galla-2 is a partner of Mms19, Galla–Xpd interaction might also affect CAK to regulate the stability of Klp61F and spindle microtubules.

An intriguing question is how Crb is related to Galla and Xpd. Maternal knockdown of Crb reduces the level of Galla-1, and *crb RNAi* mitotic phenotypes are suppressed by Galla-1 overexpression (Yeom et al., 2015). Hence, Crb seems to be required to maintain the level of Galla proteins. Conversely, Crb levels were also reduced by knockdown of Galla-2 or Xpd (Fig. S8), indicating that the levels of CGX proteins are inter-dependent. Crb loss-of-function and overexpression share similar phenotypes in nuclear division (Yeom et al., 2015). In Hippo signaling, Crb^{intra} overexpression leads to downregulation of Expanded (Ex), an upstream regulator of Hippo signaling, thus enhancing transcriptional activity of Yki (Ribeiro et al., 2014). In contrast, Ex cannot be recruited to Crb in the absence of Crb. Hence, Crb^{intra} overexpression and loss of Crb both result in overgrowth through distinct mechanisms. Crb^{intra} overexpression and *crb RNAi* in syncytial embryos also cause similar mitotic phenotypes, with a decrease in Klp61F levels (Fig. S5A). Hence, although the underlying mechanism is currently unknown, proper levels of Crb seem to be critical for the regulation of Klp61F levels.

The intracellular domain of Crb interacts with Stardust (Sdt) and Par-6 complex proteins to maintain apical–basal epithelial cell polarity (Hong et al., 2001; Bachmann et al., 2001; Nam and Choi, 2003). Maternal knockdown of Sdt or Par-6 did not significantly affect mitotic nuclei in syncytial embryos, suggesting that Crb might not function together with these proteins for syncytial mitosis (Fig. S7). However, apical localization of Crb in embryonic epithelia is regulated by endosomal trafficking (Roeth et al., 2009). Because endosomes are known to play roles for the organization of astral microtubules and chromosome alignment during mitosis (Capalbo et al., 2011; Das et al., 2014; Hehnly and Doxsey, 2014), it would be worth investigating whether endosomes might be involved in linking Crb with spindles during mitosis.

Related roles of CGX and Klp61F in eye and syncytial embryo

An initial finding in this study was a strong genetic interaction between Crb and Klp61F in the eye. It is an open question whether the functional relationships between CGX proteins and Klp61F are similar in the two distinct developmental processes; eye development and nuclear division in the syncytial embryo. As discussed above, Crb function might be mediated sequentially through Galla-2 and Xpd to regulate the levels of Klp61F for nuclear division in syncytial embryos. Because the small-eye phenotype of *Xpd RNAi* was suppressed by overexpression of Klp61F, the relationship between Xpd and Klp61F seems to be conserved in both eye and embryo development. As in the embryo, Galla-2 overexpression was unable to suppress *Xpd RNAi* phenotype in the eye.

Despite the similar relationship between Galla-2, Xpd and Klp61F in embryo nuclear division and eye development, there is an interesting difference in their genetic interaction with Crb^{intra} overexpression. The Crb^{intra} eye phenotype was suppressed by Klp61F overexpression, similarly to the rescue effect seen in the embryo. Remarkably, the same Crb^{intra} eye phenotype is suppressed by reducing Galla-2 (Yeom et al., 2015), suggesting an interesting outcome that Crb^{intra} overexpression has an opposite relationship with Galla-2 in eye development. This apparent discrepancy might be partly explained by the differences in tissues. Crb^{intra} overexpression induces overgrowth in imaginal discs by inhibiting Hippo signaling (Chen et al., 2010; Ribeiro et al., 2014) and also impairs epithelial integrity (Tepass et al., 1990). Crb^{intra} might not have such effects in syncytial embryos since epithelia have not yet formed. Because the Crb^{intra} eye phenotype is suppressed by reducing Galla-2, the dominant effects of Crb^{intra} might depend on eye-specific interaction with Galla-2.

This work provides evidence for the roles of Crb, Galla-2 and Xpd in regulating the level of Klp61F in mitosis and for their functions in eye development. Klp61F and its mammalian homolog Eg5 are conserved motor proteins that play a key role for bipolar spindle formation in mitosis. It remains to be seen whether MIP18 and XPD of the MMXD complex might participate in the regulation of Eg5 protein levels for chromosome segregation and organ growth.

MATERIALS AND METHODS

Drosophila genetics

All *Drosophila* strains were grown and maintained at room temperature unless stated otherwise. For overexpression of Crb^{intra} in differentiating eye, *UAS-*Crb^{intra} was crossed with *GMR-Gal4* (Bloomington) at 25°C. Two *UAS-Klp61F RNAi* lines (v52548, BL35804) are from the Vienna Drosophila Resource Center (VDRC) and the Bloomington Drosophila Stock Center (BDSC), respectively. *Klp61F-GFP* (BL35509, BL35510) and *klp61F*^{06345} (BL32012), *klp61F*^{07012} (BL11710) mutant lines are from the BDSC. *UAS-Klp61F* line was generated by injecting *pUASTattB-Klp61F* (Bestgene, USA). *galla-2 RNAi* lines are from VDRC (v110611) and BDSC (58320). *Xpd RNAi* lines (106998, 41021) are from VDRC. For knockdown of Xpd, *UAS-Xpd RNAi* was crossed with *ey-Gal4* (BDSC). For maternal knockdown, *crb RNAi* (BL40869, 38903), *Xpd RNAi*, *galla-2 RNAi*, *sdt RNAi* (v29844) or *par-6 RNAi* (v108560, v19732) lines were crossed with *mat-Gal4* (BDSC 7062, 7063). Proteasome mutants *Rpt*^{504210b} (BL11625) and *pros*$\beta6^{1}$ (BL6182) are from BDSC.

Generation of Klp61F and Galla-2 antibodies

An antibody against Klp61F was raised in rabbits using GST–Klp61F$^{801–1066}$ (GST tagged amino acids 806–1066), and anti-Galla-2 antibody was raised in rats with GST–Galla-2$^{1–156}$ expressed in *Escherichia coli* by isopropyl β-D-1-thiogalactopyranoside induction. Antibody production and purification were carried out by ABclonal (China). Purified Klp61F antibody was used for immunoblotting (1:1000) and immunohistochemistry (1:200). Purified Galla-2 antibody was used for immunoblotting (1:500) and immunohistochemistry (1:100).

Genetic crosses for embryo collection

To knock down maternal gene products in syncytial embryos, *maternal-Gal4* females were crossed with *UAS-RNAi* lines. F1 females (*mat>UAS RNAi*) were crossed with *UAS-GFP*, and F2 embryos were analyzed. RNAi phenotypes were not detected when *mat-Gal4* males were used for mating. For maternal overexpression of Klp61F, F1 generation females (*mat>UAS-RNAi*) were crossed with homozygote *Ubi-Klp61F GFP*, and F2 embryos were analyzed.

Immunostaining of embryos and S2 cells

Embryos laid on grape juice egg-laying plates for 2 h were collected using TXN embryo wash buffer (7% NaCl and 0.5% Triton X-100). Embryos were dechorionated using 50% bleach and moved into a 4 ml sample vial. 1 ml of heptane (Sigma) and methanol (Merck) were used to remove the vitelline membrane. After removing all solutions, embryos were stored in methanol at 4°C. For anti-tubulin staining, methanol fixation was performed to preserve microtubule structures. For embryo staining, embryos were incubated in PBS containing 0.2% saponin for 10 min. Primary antibodies were diluted in PBS containing 0.2% saponin and 0.5% normal goat serum and incubated overnight at 4°C. After washing with PBS containing 0.2% saponin four times, embryos were incubated with secondary antibodies overnight at 4°C.

Drosophila S2 cells were cultured in M3 medium (Sigma) with 10% insect medium supplement (Sigma). S2 cells were transfected with plasmid for pAc 5.1 2X Myc-Xpd and pAc 5.1 GFP Klp61F (ThermoFisher, V411020). For S2 cell staining, S2 cells were fixed in PBS containing 2% paraformaldehyde for 15 min and washed with cold PBS three times. Primary antibodies were diluted in PBS containing 0.1% saponin and 1% normal goat serum and cells were incubated overnight at 4°C. After washing with cold PBS two times, cells were incubated in secondary antibodies at room temperature for 2 h.

The following antibodies were used for embryo and S2 cell staining at indicated conditions: mouse anti-α-tubulin at 1:100 (Sigma, T9026), rat anti-Crb at 1:50 (Bhat et al., 1999), rat anti-Galla-2 at 1:100, rabbit anti-Klp61F at 1:200, rabbit anti-Myc 1:200 (Abcam, ab9106), and mouse anti-GFP 1:100 (Abcam, ab1218). Secondary antibodies conjugated with Cy3, Cy5 or FITC were from Alexa Fluor (Molecular Probes). Vectashield with DAPI (H-1200, Vector Laboratories) was used for mounting samples. Fluorescence images were acquired using Carl Zeiss LSM710 confocal microscope using a 20× or 40× objective.

GST pulldown assays

For GST pulldown, IPTG-inducible R2 cells (BL21 derivative) were transformed with MBP–Klp61F, MBP–Klp64D (Vuong et al., 2014), GST–Xpd and GST–Crb^{intra}. Bacterial cell lysates were prepared as described previously (Frangioni and Neel, 1993). The buffer used for pulldown was 20 mM Tris-HCl pH 7.5, 150 mM NaCl, 0.5 mM EDTA, 10% glycerol, 0.1% Triton X-100, 1 mM DTT and protease inhibitor cocktail (Complete EDTA-free protease inhibitor cocktail, Roche). For western blotting, rabbit anti-MBP antibody (NEB, E8030S, 1:10,000) and secondary anti-rabbit HRP-conjugated antibody (Jackson, 711-035-151, 1:10,000) were used.

Cell culture, transfection, immunoprecipitation and western blot analysis

Transfection was carried out with Cellfectin II reagent (Invitrogen) according to manufacturer's instructions. A total of 1–2 µg of DNA was used for each transfection. For immunoprecipitation (IP), cells were lysed in 0.1% CHAPS buffer (0.1% CHAPS, 10 mM NaCl, 2 mM HEPES, 0.1 mM EDTA, 0.04% PMSF and protease inhibitor cocktail) and the lysates were precleared by incubating with Protein G–sepharose beads (Amersham Bioscience) for 1 h at 4°C. Precleared lysates were immunoprecipitated with anti-Myc (Abcam, ab9106; 1:1000) at 4°C overnight. The immunoprecipitates captured by Protein G–sepharose were washed and subjected to SDS–PAGE as described previously (Vuong et al., 2014). Western blots were immunostained with anti-Flag (Sigma, F1804, 1:1000) and anti-Myc antibodies. Blots were incubated with primary antibodies overnight at 4°C. After washing with TBST (Tris-buffered saline and Tween 20) solution three times for 10 min each, blots were incubated with anti-mouse IgG (Jackson, 715-035-151, 1:10,000) or anti-rabbit IgG (Jackson, 711-035-151, 1:10,000) HRP-conjugated antibodies for 2 h at room temperature.

Embryos used for IP were dechorionated with 50% bleach, frozen in PBS and stored at −20°C. To collect adult heads for IP, whole flies were frozen in liquid nitrogen, and heads were separated with a blade. Heads and embryos were ground in lysis buffer (20 mM HEPES, 2.5 mM EDTA, 1 mM DTT, 5% glycerol, 100 mM KCl, 0.05% Triton X-100 and protease inhibitor cocktail). Embryo lysates were precleared by incubating with SureBeads Protein G magnetic beads (Bio-Rad) for 1 h at 4°C. Precleared lysates were immunoprecipitated with anti-Klp61F, anti-Galla-2 or anti-GFP (Abcam, ab1218) antibodies (1:100) at 4°C overnight. Immunoprecipitated lysates were washed with lysis buffer and subjected to SDS–PAGE. Western blots were stained with anti-Klp61F, anti-Galla-2 and anti-GFP (Abcam, ab290, 1:1000) as described above.

Embryos for western blotting experiments were collected using the same method used for IP. Embryos were lysed using a homogenizer in 1× SDS sample buffer (50mM Tris-HCl, 100mM dithiothreitol, 2% SDS, 0.1% Bromophenol Blue and 10% glycerol), boiled at 94°C for 5 min and loaded for SDS–PAGE and western blotting.

Proteins extracted from S2 cells and embryos were fractionated by SDS–PAGE and transferred onto nitrocellulose membrane. Membrane was blocked by 5% skim milk (BD Biosciences) in TBST. Western blots were stained with mouse anti-Flag (Sigma, F1804, 1:1000), rabbit anti-Myc (Abcam, ab9106, 1:1000), mouse anti-V5 (Invitrogen, R960-25, 1:1000), rabbit anti-Klp61F (1:1000), rat anti-Galla-2 (1:500) as described above.

Statistical analysis

Statistical analyses were performed by unpaired one-tailed Student's *t*-test using Microsoft Office Excel. All experiments were performed at least three times. *P*-values of <0.05 were considered as statistically significant (*P<0.05, **P<0.01, ***P<0.001).

Acknowledgements

We thank Dr Kyung-Ok Cho for critical comments on the manuscript. We acknowledge the Bloomington Drosophila Stock Center, the National Institute of Genetics stock center, the Vienna Drosophila Resource Center, the Drosophila Genomics Resource Center and the Developmental Studies Hybridoma Bank for *Drosophila* stocks and antibodies.

Competing interests

The authors declare no competing or financial interests.

Author contributions

Investigation: J.-H.H., L.T.V.; Writing - original draft: J.-H.H., L.T.V., K.-W.C.; Writing - review & editing: J.-H.H., L.T.V., K.-W.C.; Supervision: K.-W.C.

Funding

This research was supported by a National Research Laboratory grant (NRF-2011-0028326) and a Global Research Laboratory grant (2014K1A1A2042982) through the National Research Foundation of Korea, funded by the Korean Ministry of Education, Science and Technology.

Supplementary information

Supplementary information available online at
http://jcs.biologists.org/lookup/doi/10.1242/jcs.246801.supplemental

Peer review history

The peer review history is available online at
https://jcs.biologists.org/lookup/doi/10.1242/jcs.246801.reviewer-comments.pdf

References

Acar, S., Carlson, D. B., Budamagunta, M. S., Yarov-Yarovoy, V., Correia, J. J., Niñonuevo, M. R., Jia, W., Tao, L., Leary, J. A., Voss, J. C. et al. (2013). The bipolar assembly domain of the mitotic motor kinesin-5. *Nat. Commun.* **4**, 1343. doi:10.1038/ncomms2348

Bachmann, A., Schneider, M., Theilenberg, E., Grawe, F. and Knust, E. (2001). Drosophila Stardust is a partner of Crumbs in the control of epithelial cell polarity. *Nature* **414**, 638. doi:10.1038/414638a

Bhat, M. A., Izaddoost, S., Lu, Y., Cho, K.-O., Choi, K.-W. and Bellen, H. J. (1999). Discs lost, a novel multi-PDZ domain protein, establishes and maintains epithelial polarity. *Cell* **96**, 833-845. doi:10.1016/S0092-8674(00)80593-0

Brust-Mascher, I., Sommi, P., Cheerambathur, D. K. and Scholey, J. M. (2009). Kinesin-5-dependent poleward flux and spindle length control in Drosophila embryo mitosis. *Mol. Biol. Cell* **20**, 1749-1762. doi:10.1091/mbc.e08-10-1033

Capalbo, L., D'avino, P. P., Archambault, V. and Glover, D. M. (2011). Rab5 GTPase controls chromosome alignment through lamin disassembly and relocation of the NuMA-like protein Mud to the poles during mitosis. *Proc. Natl. Acad. Sci. USA*, **108**, 17343-17348. doi:10.1073/pnas.1103720108

Cheerambathur, D. K., Brust-Mascher, I., Civelekoglu-Scholey, G. and Scholey, J. M. (2008). Dynamic partitioning of mitotic kinesin-5 cross-linkers between microtubule-bound and freely diffusing states. *J. Cell Biol.* **182**, 429-436. doi:10.1083/jcb.200804100

Chen, J., Larochelle, S., Li, X. and Suter, B. (2003). Xpd/Ercc2 regulates CAK activity and mitotic progression. *Nature* **424**, 228-232. doi:10.1038/nature01746

Chen, C.-L., Gajewski, K. M., Hamaratoglu, F., Bossuyt, W., Sansores-Garcia, L., Tao, C. and Halder, G. (2010). The apical-basal cell polarity determinant Crumbs regulates Hippo signaling in Drosophila. *Proc. Natl. Acad. Sci. USA* **107**, 15810-15815. doi:10.1073/pnas.1004060107

Cole, D. G., Saxton, W. M., Sheehan, K. B. and Scholey, J. M. (1994). A "slow" homotetrameric kinesin-related motor protein purified from Drosophila embryos. *J. Biol. Chem.* **269**, 22913-22916.

Das, S., Hehnly, H. and Doxsey, S. (2014). A new role for Rab GTPases during early mitotic stages. *Small GTPases* **5**, e29565. doi:10.4161/sgtp.29565

Egly, J. M. and Coin, F. (2011). A history of TFIIH: two decades of molecular biology on a pivotal transcription/repair factor. *DNA Repair* **10**, 714-721. doi:10.1016/j.dnarep.2011.04.021
Foe, V. E. and Alberts, B. M. (1983). Studies of nuclear and cytoplasmic behaviour during the five mitotic cycles that precede gastrulation in Drosophila embryogenesis. *J. Cell Sci.* **61**, 31-70.
Frangioni, J. V. and Neel, B. G. (1993). Solubilization and purification of enzymatically active glutathione S-transferase (pGEX) fusion proteins. *Anal. Biochem.* **210**, 179-187. doi:10.1006/abio.1993.1170
Garcia, K., Stumpff, J., Duncan, T. and Su, T. T. (2009). Tyrosines in the Kinesin-5 head domain are necessary for phosphorylation by wee1 and for mitotic spindle integrity. *Curr. Biol.* **19**, 1670-1676. doi:10.1016/j.cub.2009.08.013
Goshima, G. and Vale, R. D. (2003). The roles of microtubule-based motor proteins in mitosis: comprehensive RNAi analysis in the Drosophila S2 cell line. *J. Cell Biol.* **162**, 1003-1016. doi:10.1083/jcb.200303022
Grzeschik, N. A. and Knust, E. (2005). IrreC/rst-mediated cell sorting during Drosophila pupal eye development depends on proper localisation of DE-cadherin. *Development* **132**, 2035-2045. doi:/10.1242/dev.01800
Heck, M. M., Pereira, A., Pesavento, P., Yannoni, Y., Spradling, A. C. and Goldstein, L. S. (1993). The kinesin-like protein KLP61F is essential for mitosis in Drosophila. *J. Cell Biol.* **123**, 665-679. doi:10.1083/jcb.123.3.665
Hehnly, H. and Doxsey, S. (2014). Rab11 endosomes contribute to mitotic spindle organization and orientation. *Dev. Cell* **28**, 497-507. doi:10.1016/j.devcel.2014.01.014
Hildebrandt, E. R. and Hoyt, M. A. (2000). Mitotic motors in Saccharomyces cerevisiae. *Biochim. Biophys. Acta* **1496**, 99-116. doi:10.1016/S0167-4889(00)00012-4
Hong, Y., Stronach, B., Perrimon, N., Jan, L. Y. and Jan, Y. N. (2001). Drosophila Stardust interacts with Crumbs to control polarity of epithelia but not neuroblasts. *Nature* **414**, 634-638. doi:10.1038/414634a
Hong, Y., Ackerman, L., Jan, L. Y. and Jan, Y.-N. (2003). Distinct roles of Bazooka and Stardust in the specification of Drosophila photoreceptor membrane architecture. *Proc. Natl. Acad. Sci. USA* **100**, 12712-12717. doi:10.1073/pnas.2135347100
Ito, S., Tan, L. J., Andoh, D., Narita, T., Seki, M., Hirano, Y., Narita, K., Kuraoka, I., Hiraoka, Y. and Tanaka, K. (2010). MMXD, a TFIIH-independent XPD-MMS19 protein complex involved in chromosome segregation. *Mol. Cell* **39**, 632-640. doi:10.1016/j.molcel.2010.07.029
Izaddoost, S., Nam, S.-C., Bhat, M. A., Bellen, H. J. and Choi, K.-W. (2002). Drosophila Crumbs is a positional cue in photoreceptor adherens junctions and rhabdomeres. *Nature* **416**, 178-183. doi:10.1038/nature720
Kapitein, L. C., Peterman, E. J., Kwok, B. H., Kim, J. H., Kapoor, T. M. and Schmidt, C. F. (2005). The bipolar mitotic kinesin Eg5 moves on both microtubules that it crosslinks. *Nature* **435**, 114-118. doi:10.1038/nature03503
Kashina, A. S., Scholey, J. M., Leszyk, J. D. and Saxton, W. M. (1996). An essential bipolar mitotic motor. *Nature* **384**, 225. doi:10.1038/384225a0
Kashina, A. S., Rogers, G. C. and Scholey, J. M. (1997). The bimC family of kinesins: essential bipolar mitotic motors driving centrosome separation. *Biochim. Biophys. Acta* **1357**, 257-271. doi:10.1016/S0167-4889(97)00037-2
Li, X., Urwyler, O. and Suter, B. (2010). Drosophila Xpd regulates Cdk7 localization, mitotic kinase activity, spindle dynamics, and chromosome segregation. *PLoS Genet.* **6**, e1000876. doi:10.1371/journal.pgen.1000876
Ling, C., Zheng, Y., Yin, F., Yu, J., Huang, J., Hong, Y., Wu, S. and Pan, D. (2010). The apical transmembrane protein Crumbs functions as a tumor suppressor that regulates Hippo signaling by binding to expanded. *Proc. Natl. Acad. Sci. USA* **107**, 10532-10537. doi:10.1073/pnas.1004279107
Martin-Belmonte, F. and Perez-Moreno, M. (2012). Epithelial cell polarity, stem cells and cancer. *Nat. Rev. Cancer* **12**, 23-38. doi:10.1038/nrc3169
Mazumdar, A. and Mazumdar, M. (2002). How one becomes many: blastoderm cellularization in *Drosophila melanogaster*. *Bioessays* **24**, 1012-1022. doi:10.1002/bies.10184
Mazumdar, M. and Misteli, T. (2005). Chromokinesins: multitalented players in mitosis. *Trends Cell Biol.* **15**, 349-355. doi:10.1016/j.tcb.2005.05.006
Nag, R. N., Niggli, S., Sousa-Guimarães, S., Vazquez-Pianzola, P. and Suter, B. (2018). Mms19 is a mitotic gene that permits Cdk7 to be fully active as a Cdk-activating kinase. *Development* **145**, dev156802. doi:10.1242/dev.156802
Nam, S.-C. and Choi, K.-W. (2003). Interaction of Par-6 and Crumbs complexes is essential for photoreceptor morphogenesis in Drosophila. *Development* **130**, 4363-4372. doi:10.1242/dev.00648
Pellikka, M., Tanentzapf, G., Pinto, M., Smith, C., Mcglade, C. J., Ready, D. F. and Tepass, U. (2002). Crumbs, the Drosophila homologue of human CRB1/RP12, is essential for photoreceptor morphogenesis. *Nature* **416**, 143-149. doi:10.1038/nature721
Pocha, S. M. and Knust, E. (2013). Complexities of Crumbs function and regulation in tissue morphogenesis. *Curr. Biol.* **23**, R289-R293. doi:10.1016/j.cub.2013.03.001
Pocha, S. M., Shevchenko, A. and Knust, E. (2011). Crumbs regulates rhodopsin transport by interacting with and stabilizing myosin V. *J. Cell Biol.* **195**, 827-838. doi:10.1083/jcb.201105144
Ribeiro, P., Holder, M., Frith, D., Snijders, A. P. and Tapon, N. (2014). Crumbs promotes expanded recognition and degradation by the SCF(Slimb/β-TrCP) ubiquitin ligase. *Proc. Natl. Acad. Sci. USA* **111**, E1980-E1989. doi:10.1073/pnas.1315508111
Robinson, B. S., Huang, J., Hong, Y. and Moberg, K. H. (2010). Crumbs regulates Salvador/Warts/Hippo signaling in Drosophila via the FERM-domain protein expanded. *Curr. Biol.* **20**, 582-590. doi:10.1016/j.cub.2010.03.019
Roeth, J. F., Sawyer, J. K., Wilner, D. A. and Peifer, M. (2009). Rab11 helps maintain apical Crumbs and adherens junctions in the Drosophila embryonic ectoderm. *PLoS One* **4**, e7634. doi:10.1371/journal.pone.0007634
Saunders, A. M., Powers, J., Strome, S. and Saxton, W. M. (2007). Kinesin-5 acts as a brake in anaphase spindle elongation. *Curr. Biol.* **17**, R453-R454. doi:10.1016/j.cub.2007.05.001
Scholey, J. M. (2009). Kinesin-5 in Drosophila embryo mitosis: sliding filament or spindle matrix mechanism? *Cell Motil. Cytoskeleton* **66**, 500-508. doi:10.1002/cm.20349
Sharp, D. J., Mcdonald, K. L., Brown, H. M., Matthies, H. J., Walczak, C., Vale, R. D., Mitchison, T. J. and Scholey, J. M. (1999). The bipolar kinesin, KLP61F, cross-links microtubules within interpolar microtubule bundles of Drosophila embryonic mitotic spindles. *J. Cell Biol.* **144**, 125-138. doi:10.1083/jcb.144.1.125
Tepass, U. (2012). The apical polarity protein network in Drosophila epithelial cells: regulation of polarity, junctions, morphogenesis, cell growth, and survival. *Annu. Rev. Cell Dev. Biol.* **28**, 655-685. doi:10.1146/annurev-cellbio-092910-154033
Tepass, U., Theres, C. and Knust, E. (1990). Crumbs encodes an EGF-like protein expressed on apical membranes of Drosophila epithelial cells and required for organization of epithelia. *Cell* **61**, 787-799. doi:10.1016/0092-8674(90)90189-L
Vale, R. D. and Milligan, R. A. (2000). The way things move: looking under the hood of molecular motor proteins. *Science* **288**, 88-95. doi:10.1126/science.288.5463.88
Vuong, L. T., Mukhopadhyay, B. and Choi, K. W. (2014). Kinesin-II recruits Armadillo and Dishevelled for wingless signaling in Drosophila. *Development* **141**, 3222-3232. doi:10.1242/dev.106229
Waitzman, J. S. and Rice, S. E. (2014). Mechanism and regulation of kinesin-5, an essential motor for the mitotic spindle. *Biol. Cell* **106**, 1-12. doi:10.1111/boc.201300054
Wilson, P. G., Fuller, M. T. and Borisy, G. G. (1997). Monastral bipolar spindles: implications for dynamic centrosome organization. *J. Cell Sci.* **110**, 451-464. doi:10.1002/bies.950190603
Yeom, E., Hong, S. T. and Choi, K. W. (2015). Crumbs interacts with Xpd for nuclear division control in Drosophila. *Oncogene* **34**, 2777-2789. doi:10.1038/onc.2014.202
Zurita, M. and Merino, C. (2003). The transcriptional complexity of the TFIIH complex. *Trends Genet.* **19**, 578-584. doi:10.1016/j.tig.2003.08.005

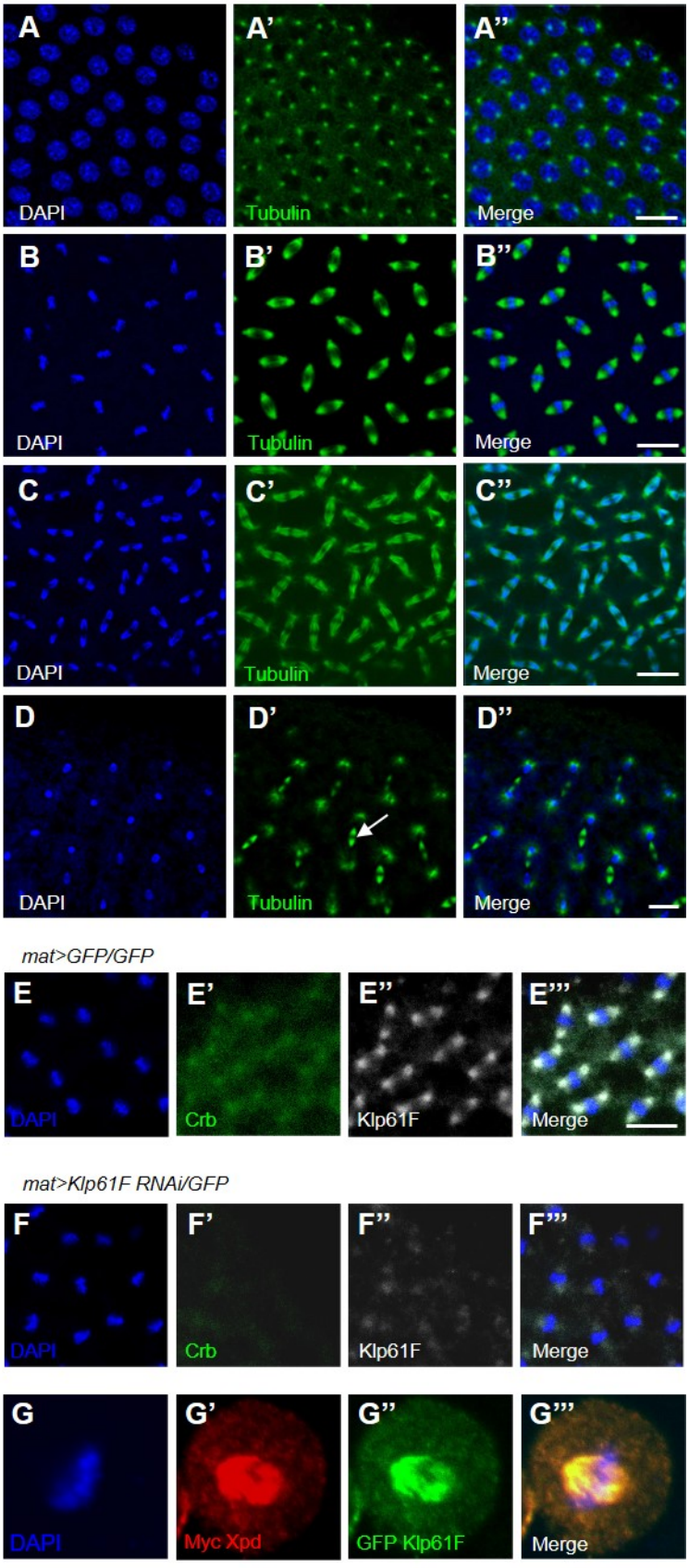

Figure S1. Localization of Tubulin during nuclear division and effect of *Klp61F RNAi*

(A-D) Pattern of Tubulin in embryos at nuclear division cycle 11. Scale bar, 20μm. (A-D) Localization of Tubulin. (A) Tubulin is localized in spindle poles during prophase. (B-C) Tubulin shows spindle pattern in meta- and anaphase. (D) Tubulin is enriched in midbody during telophase (arrows). (E-F) Effects of *Klp61F RNAi* on Crb. (E-E’’’) *mat>GFP* control embryos were stained with Crb and Klp61F in the absence of anti-Tubulin antibody. Both Crb and Klp61F show tubulin pattern. Scale bar, 20μm. (F-F’’’) Crb and Klp61F levels are decreased in Klp61F knockdown condition. (G-G’’’) Localization of Klp61F and Xpd in S2 cells. S2 cells were transfected by Myc-Xpd and GFP-Klp61F constructs. Both Klp61F and Xpd show tubulin pattern.

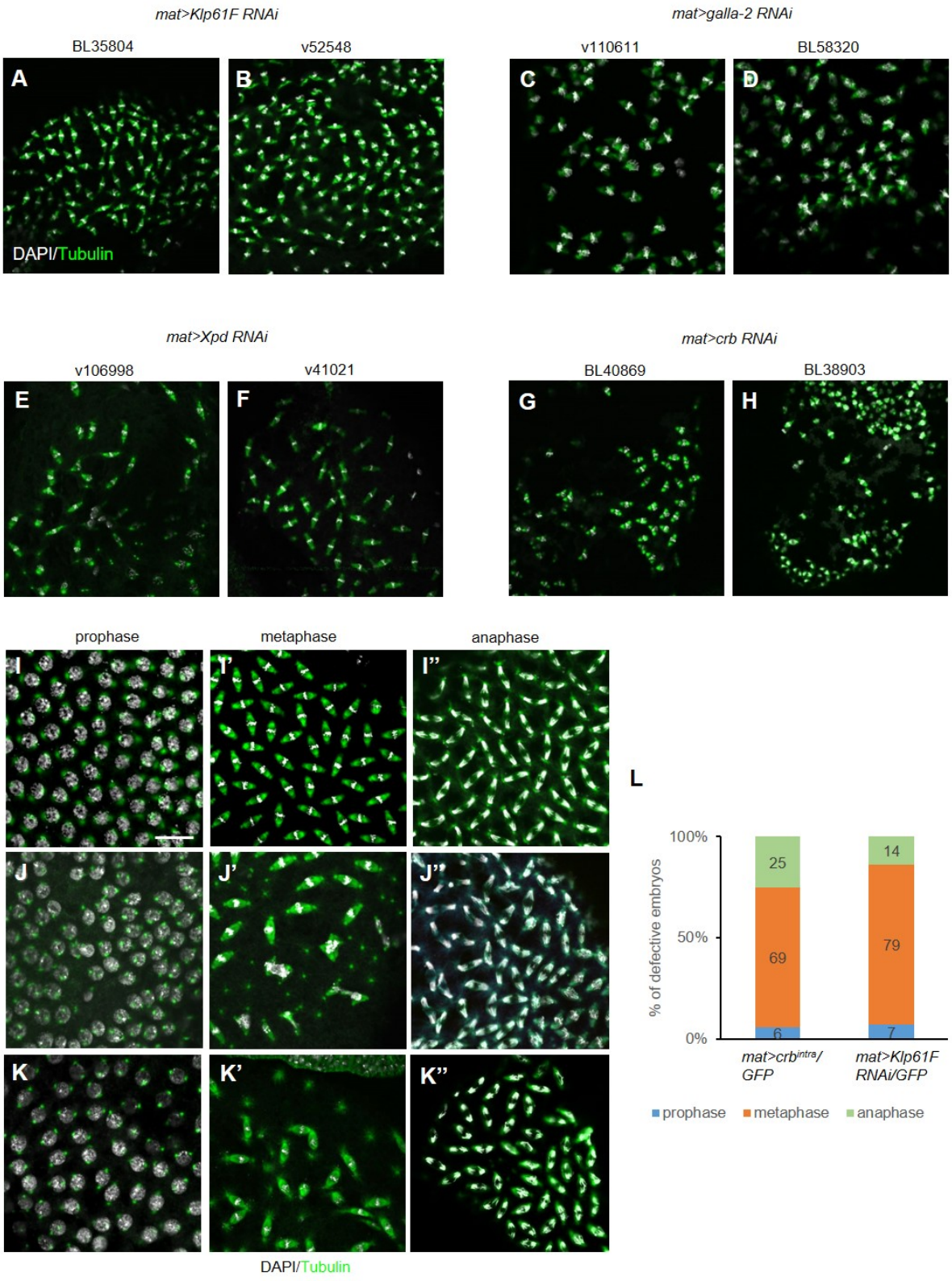

Figure S2. Mitotic defects by knockdown of Crb, Galla-2, Xpd and Klp61F

(A-H) Mitotic defects by knockdown of Crb, Galla-2, Xpd and Klp61F by *mat-Gal4*. Quantification of different phenotypes such as free centrosomes and fused spindles is shown in Fig. S6. (A-B) Independent *Klp61F RNAi* lines (BL35804, v52548). (C-D) *galla-2 RNAi*

lines (v110611, BL58320). (E-F) *Xpd RNAi* lines (v106998, v41021). (G-H) *crb RNAi* lines (BL40869, BL38903). (I-K) Dividing nuclei stained for Tubulin (green) and DAPI (white). Scale bar, 20μm. (I-I'') Wild type prophase, metaphase and anaphase. (J-J'') Prophase, metaphase and anaphase in Klp61F knockdown condition. (K-K'') Prophase, metaphase and anaphase in Crb^{intra} overexpression condition. Spindle defects were mainly detected during metaphase in both Crb^{intra} overexpression and *Klp61F* RNAi conditions. (L) The chart shows that majority of defective embryos are in metaphase. 70% of defective embryos with Crb^{intra} overexpression (n = 83) has phenotypes in metaphase. 80% of defective *Klp61F* RNAi embryos (n = 84) show phenotypes in metaphase.

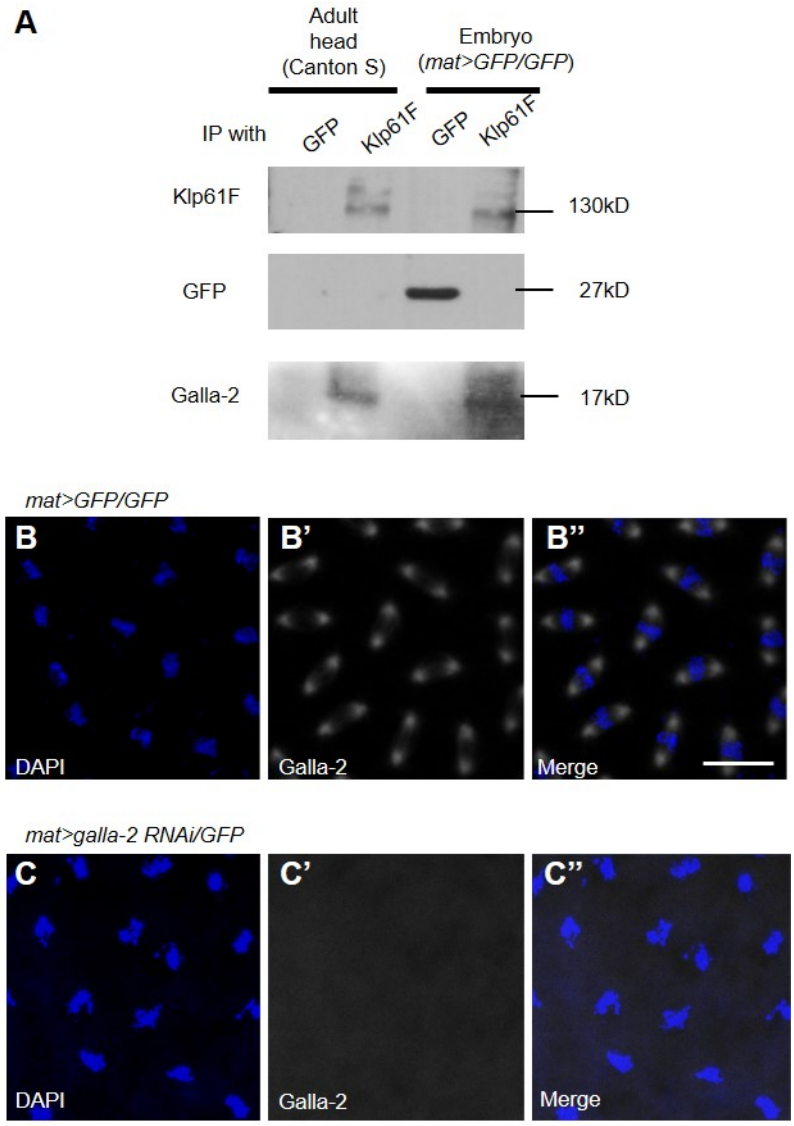

Figure S3. Endogenous IP with Klp61F and Galla-2 and effects of *galla-2 RNAi.*

(A) Lysates from adult heads (Canton S) and syncytial embryos (*mat>GFP/GFP*) were immunoprecipitated with GFP (Lanes 1 and 3), Klp61F (Lanes 2 and 4). Galla-2 was co-immunoprecipitated with Klp61F in both tissues (Lanes 2 and 4). (B-C) Immunostaining for Galla-2 in the absence of anti-Tubulin antibody. Scale bar, 20µm. (B-B'') Galla-2 pattern in control embryos (*mat>GFP*). Galla-2 staining shows similar pattern as mitotic spindles. (C-C'') In Galla-2 knockdown condition, level of Galla-2 is reduced in mitotic spindles.

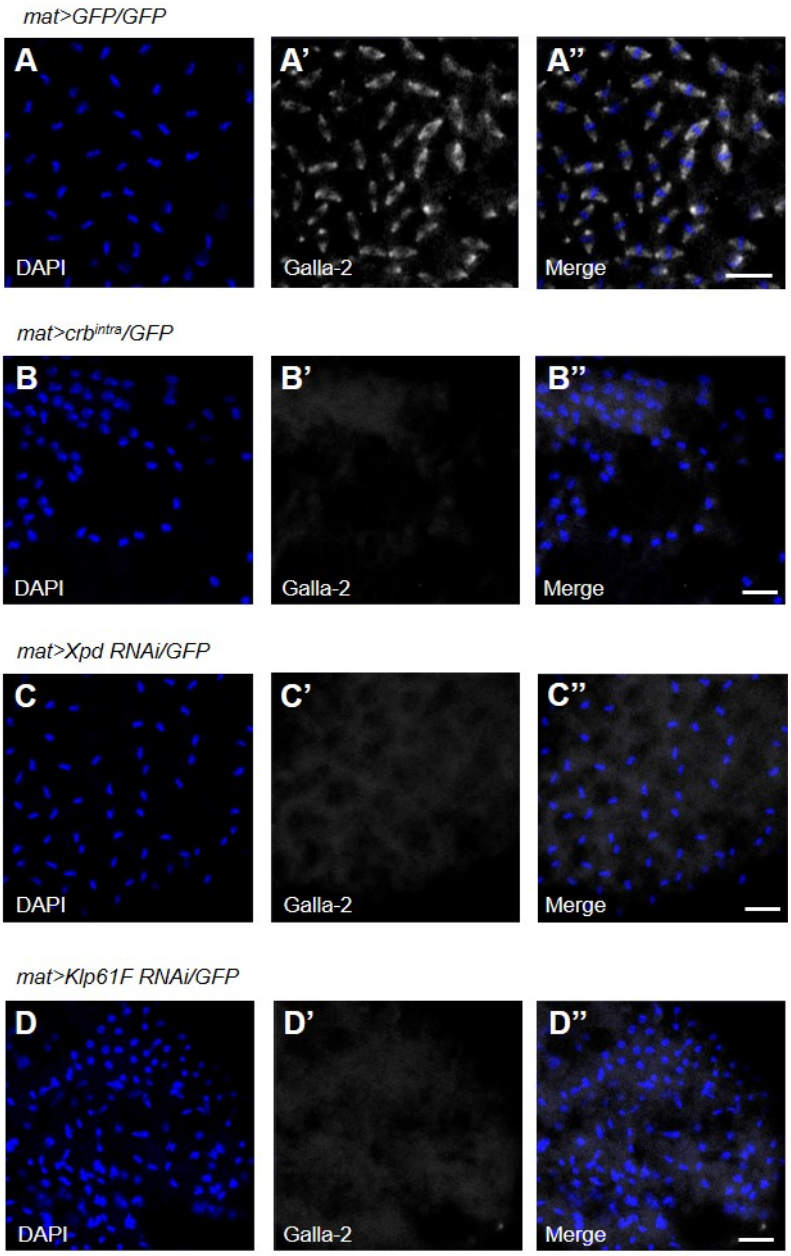

Figure S4. Effects of Crb^{intra} overexpression, *Xpd RNAi* or *Klp61F RNAi* on Galla-2 level.

(A-A'') Galla-2 staining in spindles in wild type embryos. (B-D) Strong reduction of Galla-2 by Crb^{intra} overexpression (B), *Xpd RNAi* (C), or *Klp61F RNAi* (D). Scale bar, 20μm.

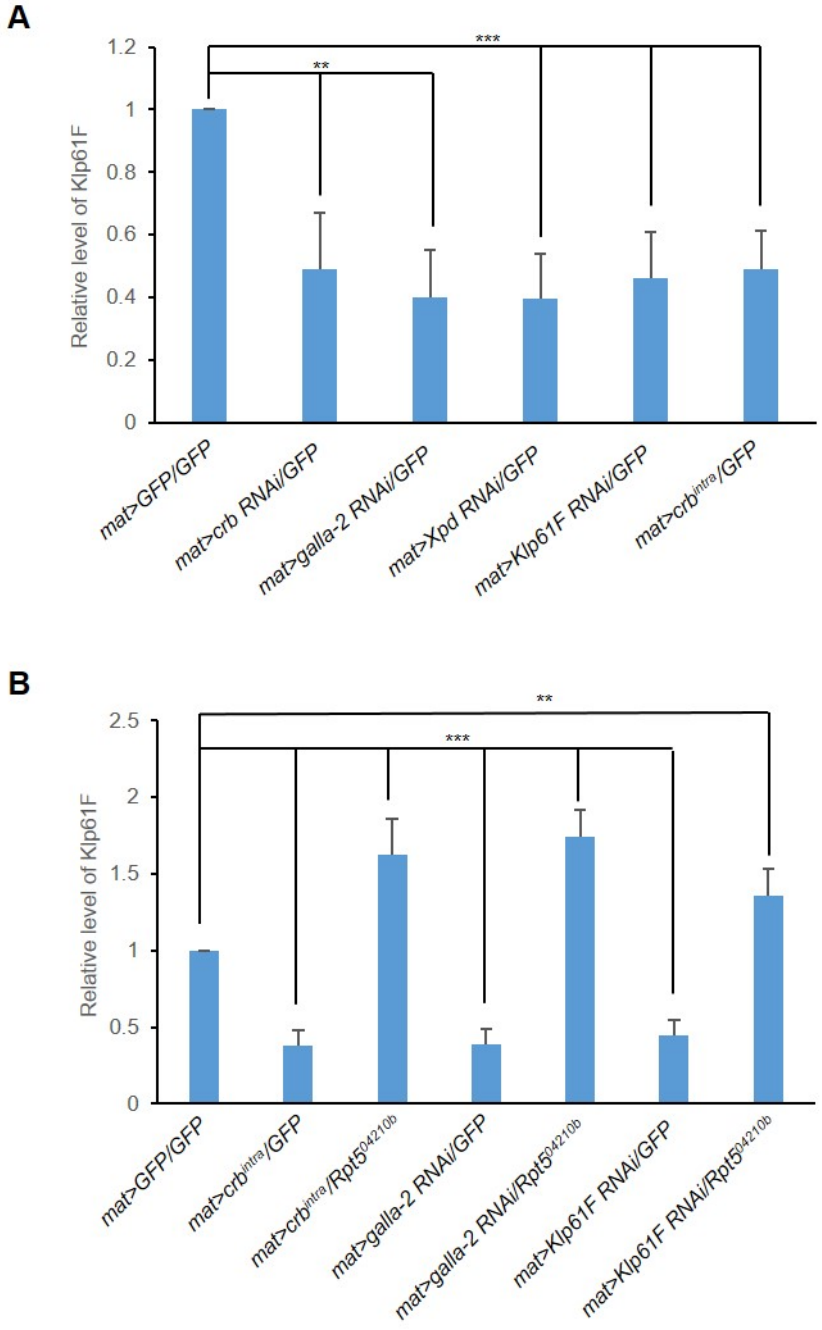

Figure S5. Quantitative analysis of Klp61F levels in embryos of different genotypes.

(A) Effects of different genotypes on the level of Klp61F in syncytial embryos. Protein extracts from embryos of indicated genotypes were separated by SDS PAGE and western blotted. Blots were immunostained for Klp61F and Tubulin. Klp61F levels relative to Tubulin were quantified. Quantification data and t-test results for 20 blots are shown in Table S1. (A) Knockdown of Crb, Galla, and Xpd or Crb^{intra} overexpression resulted in about 55% of reduction of Klp61F level. (B) Effects of a proteasome mutation ($Rpt5^{04210b}/+$) on the level of Klp61F. Protein extracts were prepared from different genotypes as indicated. Western blots

were stained for Klp61F and Tubulin as in (A). Quantification of relative Klp61F levels with statistics for 20 western blots is shown in Table S2. Crb^{intra} overexpression, *galla-2 RNAi*, and *Klp61F RNAi* result in reduction of Klp61F level. $Rpt5^{04210b}$/+ heterozygous mutation increased Klp61F level about 1.4-1.8-fold higher than the control (*mat>GFP/GFP*).

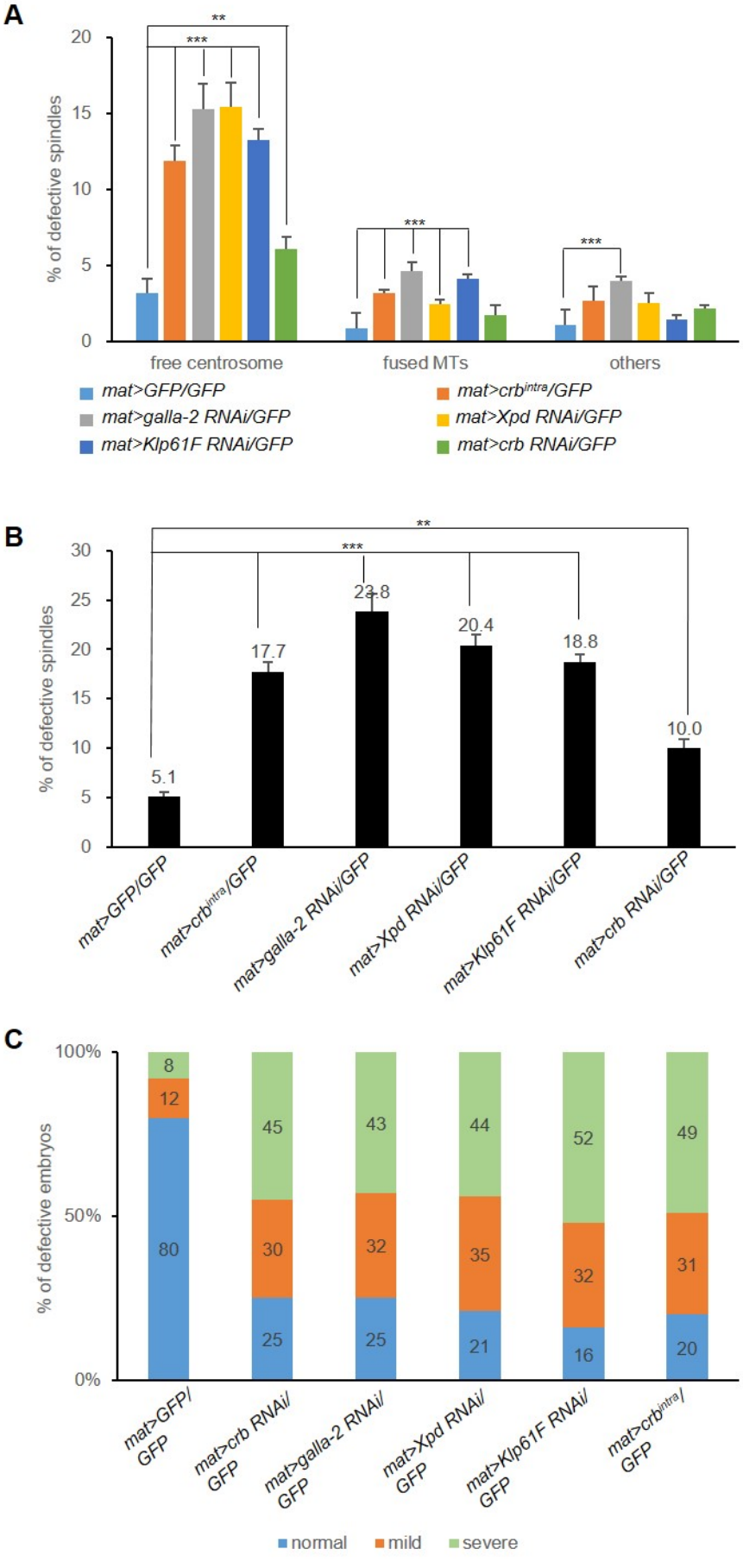

Figure S6. Quantification of spindle defects in different genotypes.

(A) Quantification of different mitotic phenotypes. Overexpression of Crb^{intra} and knockdown of Crb, Galla-2, Xpd and Klp61F by *mat-Gal4* lead to spindle defects in embryos. Spindle defects are divided into three categories: free centrosomes, fused/branched spindles, and others (mono-polar or multi-polar spindles). (B) Quantification of all mitotic phenotypes shown in (A). Each bar shows the sum of different phenotypes for indicated genotypes. Error bars are s.d. n>30. ***P<0.01* ****P<0.001* (C) Nuclear loss phenotype caused by knockdown of Crb, Galla-2, Xpd and Klp61F or Crb^{intra} overexpression. 'mild' and 'severe' means embryos showing less than 10% or more than 10% of nuclei-free area, respectively. In control (*mat>GFP/GFP*), 80% of embryos were normal while 20% of embryos showed mild or severe phenotype. About 75% of embryos showed nuclear loss phenotype in Crb^{intra} overexpression or indicated RNAi condition (n>85).

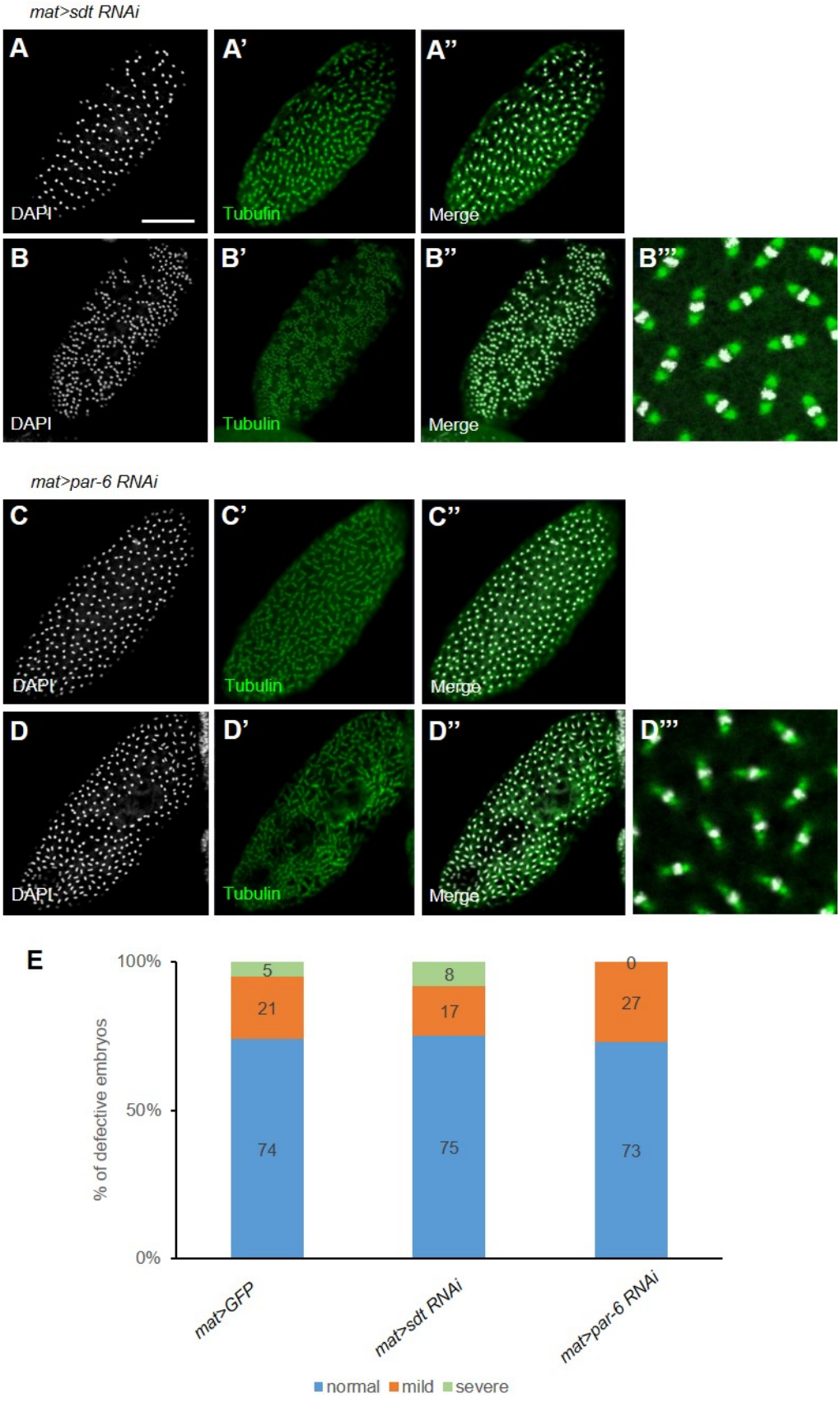

Figure S7. Effects of *sdt* and *par-6* RNAi in nuclear division

(A-B) Knockdown of Sdt. A majority of embryos show relatively normal pattern of nuclear division (A-A”). Some embryos show nuclear loss phenotypes (B-B”), but cortical nuclei show normal pattern of mitotic spindles (B”’). (C-D) Knockdown of Par-6. A majority of embryos show relatively normal pattern of nuclear division (C-C”). Some embryos show nuclear loss phenotypes (D-D”) as in (B), but cortical nuclei show normal pattern of mitotic spindles (D”’). (E) Quantification of nuclear loss phenotypes shown in (B) and (D). Both *sdt* and *par-6 RNAi* did not show significant difference from control (*mat>GFP*). Scale bar, 100μm.

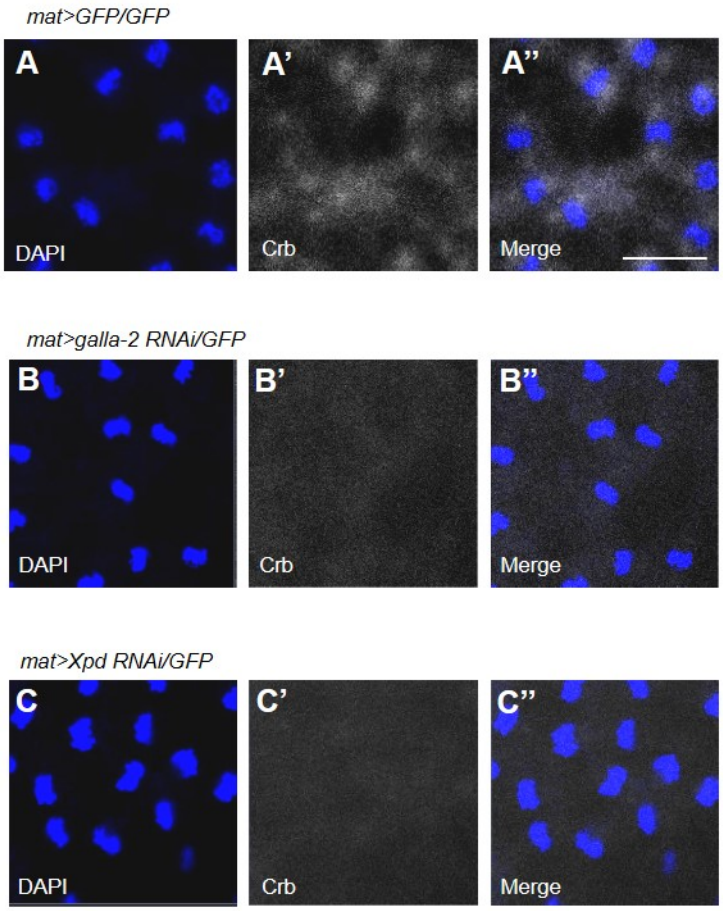

Figure S8. Effects of Galla-2 or Xpd knockdown on Crb level.

(A-A'') Localization of Crb in control embryo (*mat>GFP/GFP*). Crb is distributed in the spindle region during metaphase. Scale bar, 20μm. (B-B'') Crb level is reduced in *mat>galla-2 RNAi* condition. (C-C'') Crb level is decreased in Xpd knockdown condition.

Fig 3G	free centrosome	fused MTs	others
GFP – crb^{intra} (n=27)	***(p=0.0006)	*(p=0.0117)	**(P=0.0012)
crb^{intra} - crb^{intra}/Klp61F (n=27)	**(p=0.0062)	*(p=0.0184)	***(P=0.0004)

Fig 4D	free centrosome	fused MTs	others
GFP – galla-2 RNAi (n=25)	**(p=0.0039)	**(p=0.0012)	*(P=0.0106)
galla-2 RNAi – galla-2 RNAi/Klp61F (n=25)	**(p=0.0032)	**(p=0.0011)	**(P=0.0060)

Fig 5C	free centrosome	fused MTs	others
GFP – Xpd RNAi (n=25)	**(p=0.0050)	*(p=0.0266)	*(P=0.0319)
Xpd RNAi – Xpd RNAi/Klp61F(n=25)	**(p=0.0034)	(p=0.4684)	**(P=0.0078)

Fig 7A	free centrosome	fused MTs	others
GFP – galla-2 RNAi (n=17)	**(p=0.0015)	***(p=0.0005)	*(p=0.0141)
galla-2 RNAi – galla-2 RNAi/Rpt5^{04210b} (n=17)	**(p=0.0034)	(p=0.4684)	**(P=0.0078)
GFP – Klp61F RNAi (n=19)	**(p=0.0010)	***(p=0.0006)	**(p=0.0019)
Klp61F RNAi – klp61F RNAi/Rpt5^{04210b} (n=19)	**(p=0.0082)	*(p=0.0178)	*(p=0.0467)

Fig 7B	free centrosome	fused MTs	others
GFP – galla-2 RNAi (n=18)	***(p=0.0001)	***(p=0.0003)	**(p=0.0063)
galla-2 RNAi – galla-2 RNAi/Prosb6^{1} (n=18)	**(p=0.0015)	**(p=0.0012)	***(p=0.0007)
GFP – crb^{intra} (n=20)	**(p=0.0012)	**(p=0.0055)	(p=0.3090)
crb^{intra} – crb^{intra}/Prosb6^{1} (n=20)	***(p=0.0005)	*(p=0.0258)	(p=0.2495)

Fig 8A	free centrosome	fused MTs	others
GFP – galla-2 (n=27)	(p=0.1112)	(p=0.1724)	(p=0.4507)
GFP – Xpd RNAi (n=27)	**(p=0.0013)	***(p=0.0008)	(p=0.1223)
Xpd RNAi – Xpd RNAi/galla-2 (n=27)	*(p=0.0461)	*(p=0.0464)	(p=0.1835)

Fig 8B	free centrosome	fused MTs	others
GFP – galla-2 RNAi (n=26)	***(p=0.0004)	**(p=0.0055)	*(P=0.0210)
GFP – Xpd (n=26)	(p=0.0850)	**(p=0.0206)	***(P=0.0009)
galla-2 RNAi – galla-2 RNAi/Xpd (n=26)	***(p=0.0008)	*(p=0.0103)	*(p=0.0273)

Table S1. Statistical analysis

T-test results of each experiment shown in main figures. * p<0.05, **p<0.01, ***p<0.001

Western blots	*mat>GFP/ GFP*	*mat>crb RNAi/GFP*	*mat>galla-2 RNAi/GFP*	*mat>Xpd RNAi/GFP*	*mat>Klp61F RNAi/GFP*	*mat>crb^{intra}*
1	1	0.38	0.14	0.13	0.16	0.45
2	1	0.26	0.24	0.26	0.39	0.52
3	1	0.45	0.46	0.51	0.52	0.31
4	1	0.54	0.58	0.51	0.52	0.52
5	1	0.81	0.45	0.45	0.56	0.57
6	1	0.34	0.48	0.64	0.81	0.67
7	1	0.44	0.34	0.34	0.48	0.54
8	1	0.26	0.66	0.26	0.57	0.52
9	1	0.72	0.54	0.72	0.32	0.48
10	1	0.62	0.52	0.27	0.49	0.26
11	1	0.54	0.27	0.49	0.48	0.71
12	1	0.64	0.28	0.34	0.46	0.64
13	1	0.25	0.39	0.26	0.35	0.51
14	1	0.34	0.73	0.24	0.37	0.63
15	1	0.39	0.36	0.48	0.34	0.35
16	1	0.82	0.28	0.39	0.45	0.55
17	1	0.26	0.43	0.54	0.8	0.46
18	1	0.49	0.24	0.35	0.35	0.37
19	1	0.54	0.25	0.39	0.43	0.46
20	1	0.73	0.39	0.34	0.34	0.32
Average	1	0.491	0.4015	0.3955	0.4595	0.492
S.D		0.181	0.150	0.143	0.149	0.120

Table S2. Quantitative data for Figure S5A

Quantification of 20 Western blot assays. Data show that relative Klp61F levels normalized to Tubulin are reduced in Crb, galla-2 and Xpd knockdown or Crb^{intra} overexpression condition.

Western blots	*mat>GFP/ GFP*	*mat>crb^{intra}*	*mat>crb^{intra}/ Rpt5^{04210b}*	*mat>galla-2 RNAi/GFP*	*mat>galla-2 RNAi/Rpt5^{04210b}*	*mat>Klp61F RNAi/GFP*	*mat>Klp61F RNAi/Rpt5^{04210b}*
1	1	0.41	1.67	0.58	1.44	0.62	1.05
2	1	0.32	1.82	0.32	1.89	0.45	1.39
3	1	0.42	1.88	0.26	2.07	0.37	1.72
4	1	0.45	1.54	0.48	1.78	0.57	1.27
5	1	0.33	1.64	0.29	1.63	0.51	1.36
6	1	0.28	1.62	0.57	1.46	0.34	1.29
7	1	0.56	1.67	0.36	1.62	0.49	1.28
8	1	0.32	1.89	0.37	1.95	0.42	1.34
9	1	0.61	1.02	0.49	1.59	0.39	1.22
10	1	0.34	1.27	0.42	1.84	0.48	1.37
11	1	0.26	1.68	0.24	1.85	0.37	1.85
12	1	0.37	1.63	0.55	1.75	0.42	1.53
13	1	0.36	1.71	0.42	1.53	0.67	1.19
14	1	0.42	1.3	0.33	1.49	0.41	1.45
15	1	0.49	1.54	0.28	1.97	0.29	1.39
16	1	0.52	1.89	0.34	1.83	0.48	1.24
17	1	0.31	1.84	0.39	1.82	0.43	1.33
18	1	0.33	1.78	0.45	1.73	0.34	1.31
19	1	0.29	1.84	0.38	1.68	0.39	1.26
20	1	0.24	1.35	0.29	1.88	0.56	1.32
Average	1	0.3815	1.629	0.3905	1.74	0.45	1.358
S.D		0.099	0.230	0.100	0.175	0.096	0.174

Table S3. Quantitative data for Figure S5B

Quantification of 20 Western blot assays. Data show relative Klp61F levels normalized to Tubulin. Reduced Klp61F levels caused by Crb^{intra} overexpression or *galla-2* and *Xpd RNAi* are recovered by *Rpt5^{04210b}*/+ heterozygous mutation.